

1 ***Original Article***

2 **Label-free quantitative proteomics analyses of mouse astrocytes provides insight**

3 **into the host response mechanism at different developmental stages of**

4 ***Toxoplasma gondii***

5 Huanhuan Xie, Chao Xu, Guihua Zhao, Hongjie Dong, Lisha Dai, Haozhi Xu, Lixin

6 Zhang, Hang Sun, Qi Wang, Junmei Zhang, Kun Yin*

7 (Shandong Institute of Parasitic Diseases, Shandong First Medical University &

8 Shandong Academy of Medical Sciences, Jining, Shandong, China 272033)

9 Abbreviated Names:

10 Xie H, Xu C, Zhao G, Dong H, Dai L, Xu H, Zhang L, Sun H, Wang Q, Zhang J, Yin

11 K

12 *Address Correspondence to:

13 Kun Yin, Shandong Institute of Parasitic Diseases, Shandong First Medical University

14 & Shandong Academy of Medical Sciences, 11 Taibai Middle Road, Jining 272033,

15 China.

16 E-mail: kyin@sdfmu.edu.cn

17 Tel: 86-0537-2350605; Fax: 86-0537-2353277

18 **Abstract**

19 *Toxoplasma gondii* (*T. gondii*) is an opportunistic parasite that can infect the
20 central nervous system (CNS), causing severe toxoplasmosis and behavioral cognitive
21 impairment. Mortality is high in immunocompromised individuals with toxoplasmosis,
22 most commonly due to reactivation of infection in the CNS. There are still no effective
23 vaccines and drugs for the prevention and treatment of toxoplasmosis. There are five
24 developmental stages for *T. gondii* to complete life cycle, of which the tachyzoite and
25 bradyzoite stages are the key to the acute and chronic infection. In this study, to better
26 understanding of how *T. gondii* interacts with the host CNS at different stages of
27 infection, we constructed acute and chronic infection models of *T. gondii* in astrocytes,
28 and used label-free proteomics to detect the proteome changes before and after infection,
29 respectively. A total of 4676 proteins were identified, among which 163 differentially
30 expressed proteins (DEPs) (fold change ≥ 1.5 or ≤ 0.67 and p -value ≤ 0.05) including 109
31 up-regulated proteins and 54 down-regulated proteins in C8-TA vs C8 group, and 719
32 DEPs including 495 up-regulated proteins and 224 down-regulated proteins in C8-BR
33 vs C8-TA group. After *T. gondii* tachyzoites infected astrocytes, DEPs were enriched
34 in immune-related biological processes to promote the formation of bradyzoites and
35 maintain the balance of *T. gondii*, CNS and brain. After *T. gondii* bradyzoites infected
36 astrocytes, the DEPs up-regulated the host's glucose metabolism, and some up-
37 regulated DEPs were closely related to neurodegenerative diseases. These findings not
38 only provide new insights into the psychiatric pathogenesis of *T. gondii*, but also
39 provide potential targets for the treatment of acute and chronic Toxoplasmosis.

40 **Key words :** *Toxoplasma gondii*, acute and chronic infection, toxoplasmosis,
41 astrocytes, Label-free proteomics, differentially expressed proteins

42 1. Introduction

43 *Toxoplasma gondii* (*T. gondii*) is an obligate intracellular parasite that can infect
44 almost all warm-blooded animals, including humans and livestock, and causing
45 zoonotic parasitic diseases^[1-4]. It is estimated that 30% of the world population was
46 infected by *T. gondii*, and in China, approximately 8.2% Chinese population was
47 infected with it^[5,6]. *T. gondii* has a complex life cycle, and almost all warm-blooded
48 animals can become intermediate hosts, except for the terminal host felid. During the
49 intracellular life, *T. gondii* undergoes five developmental stages including tachyzoite,
50 bradyzoite, sporozoite, schizont, and gametocyte. Tachyzoites are parasitic in
51 pseudocyst, and bradyzoites are present in the tissue cyst. The schizont and
52 gametophyte are the sexual reproductive stages, and finally formed into oocyst. In the
53 intermediate hosts, there are two infectious stages: tachyzoite and bradyzoite. Since the
54 morphological difference between tachyzoite and bradyzoite is quite small, the
55 bradyzoite-specific expression protein BAG1 is usually used for the identification of
56 bradyzoites.

57 The mutual transformation of tachyzoites and bradyzoites is the central link in the
58 pathogenesis of *T. gondii*. Tachyzoites can cause acute infection, while bradyzoites are
59 the main cause of chronic infection. Acute toxoplasmosis is more prevalent in
60 immunodeficiency patients^[7-9]. However, when the tachyzoites are transformed into
61 bradyzoites and form cysts in normal immune responses, they will latently parasitize in
62 the host's brain and ocular chorioretinal areas. When the host's immune system is
63 impaired, the latent bradyzoites (in the CNS) could burst out of the cysts, reconvert to

64 replicative tachyzoites and triggering a new round of infection^[10]. In the chronic stages
65 of infection, the host may have alterations in behavior and cognition^[11-14]. For example,
66 in rodent hosts, the chronic infection can lead to excessive exercise, reduced anxiety,
67 reduced new phobias, and predator vigilance. In particular, *T. gondii* could induce
68 changes in rodent olfactory preferences, converting an innate aversion for cat odor into
69 attraction, in order to enhance their own transmission^[15]. Nevertheless, Boillat *et al*
70 found that *T. gondii* infection could commonly shift the host's aversion to predators,
71 which are not specific to cats. And this alternation may be related to cysts in the host
72 brain^[16]. As far as humans are concerned, a large amount of seroepidemiological data
73 have shown that *T. gondii* infection has increased the incidence of mental illness,
74 especially focus on the relationship among schizophrenia, suicide and traffic
75 accidents^[17-20].

76 *T. gondii* can infect a variety of cells in the CNS, including neuronal cells,
77 astrocytes, microglia and Purkinje cells. Studies have reported that tachyzoites in CNS
78 are more susceptible to astrocytes^[21]. Astrocytes are the most abundant glial cell type
79 in CNS, constitute a heterogeneous cell population and could maintain neural
80 homeostasis^[22]. Astrocytes play an important role including regulation of energy
81 metabolism, brain barrier, synaptic structure and plasticity^[23-26]. They can also interact
82 with CD⁴⁺ and CD⁸⁺ T cells to prevent neuronal damage^[27]. However, regulation details
83 of astrocytes infected with tachyzoites or/and bradyzoites are still unknown. Therefore,
84 exploring the response of astrocytes infected with different stages of *T. gondii* will help
85 to understand the mechanism of interaction between *T. gondii* and host CNS, and lay a

86 solid foundation for the study of acute and chronic Toxoplasmosis.

87 Therefore in this study, we have established an in vitro infected astrocytes model
88 using *T. gondii* RH strain and mouse C8-D1A astrocytes. Based on the acute infection
89 model with RH tachyzoites, we have also successfully transformed the tachyzoites into
90 bradyzoites in C8-D1A cells. By using the Label-free proteome detection, we have
91 figured out the changes of host protein expression before and after infection with
92 tachyzoite and bradyzoite, respectively. Our results revealed the molecular mechanism
93 of astrocytes to parasites at different stages of *T. gondii* infection. It can also provide
94 new insights into the pathogenic mechanism of acute and chronic toxoplasmosis, and
95 show new targets for the development of anti-*T. gondii* therapeutic drugs.

96 **2. Materials and methods**

97 **2.1 *T. gondii* and cell culture**

98 *T. gondii* tachyzoites (RH strain) were maintained using human foreskin fibroblast
99 (HFF) cells, which were cultured in DMEM supplemented with 10% fetal bovine serum
100 (FBS) and 100 IU/mL penicillin, and 100 µg/mL streptomycin at 37°C in a humidified
101 atmosphere of 5% CO₂. When the infected HFF monolayer was lysed, collected cell
102 mixture and filtered through a 5 µm filter to obtain *T. gondii* tachyzoites, counted and
103 stored at -80°C. C8-D1A mouse astrocytes were cultured under the same conditions as
104 HFF cells.

105 **2.2 Sample preparation and collection**

106 C8-D1A (5×10⁵ cells) were seeded on 8 mm coverslips in 6-well plates, and
107 cultured in 37°C with 5% CO₂. When cells formed confluent monolayers, replace

108 medium with 3% FBS. *RH* strain of *T. gondii* were added to C8-D1A (The ratio of cells
109 to tachyzoites was 10:1) for 24 h. PBS washed two times and collected samples,
110 centrifuged at 1000 g for 5 minutes, stored at -80°C, the group was named C8-TA.
111 Alkaline-induced transformation of tachyzoites in vitro were performed. The *T. gondii*
112 tachyzoites were added to cells at a ratio of 1:10 and cultured for 8 h at 37°C with 5%
113 CO₂, then continued to culture for 96 h in alkaline media (pH 8.2) and changed the
114 medium every 1-2 days. PBS washed two times and collected samples, centrifuged at
115 1000 g for 5 minutes, stored at -80°C, the group was named C8-BR. The uninfected
116 group was named C8. There were three replicates for each group, therefore 9 samples
117 were used for following experiment.

118 **2.3 RT-PCR**

119 RT-PCR was used to detect the expression of bradyzoite antigen 1 (BAG1). Total
120 RNA was extracted from C8-BR group with TRIzol (Sigma-Aldrich, USA). The
121 isolated RNA was converted to cDNA using Takara PrimerScriptTM RT reagent Kit
122 according to the instructions. BAG1 primers were as follows:

123 Forward primer: 5'-TCGCCTCTAACAGCTAGAC-3';

124 Reverse primer: 5'-CCCTGAATCCTCGACCTTGAT-3';

125 The reaction conditions were 94 °C for 5 min, 94 °C for 40 s, 56 °C for 40 s, and
126 72 °C for 1 min. PCR products were analyzed by 1% agarose gel electrophoresis.

127 **2.4 Protein extraction and trypsin digestion**

128 All of the samples were sonicated three times on ice using a high intensity
129 ultrasonic processor (Scientz) in lysis buffer (8 M urea, 1% Protease Inhibitor Cocktail).

130 Centrifuged at 12,000g at 4°C for 10 min to remove remaining debris. BCA kit was
131 used to determine the protein concentration according to the manufacturer's
132 instructions. For digestion, the protein solution of each sample was reduced with 5 mM
133 dithiothreitol for 30 min at 56 °C and then alkylated with 11 mM iodoacetamide in the
134 dark for 15 min at room temperature. 100 mM TEAB was added to dilute the sample.
135 Finally, trypsin was added for the first digestion overnight (trypsin-to-protein mass ratio
136 was 1:50) and performed a subsequent 4 h-digestion (trypsin-to-protein mass ratio was
137 1:100).

138 **2.5 LC-MS/MS Analysis**

139 The tryptic peptides were dissolved in 0.1% formic acid (solvent A), directly
140 loaded onto a home-made reversed-phase analytical column (15-cm length, 75 µm i.d.).
141 The gradient was comprised of an increase from 6% to 23% solvent B (0.1% formic
142 acid in 98% acetonitrile) over 26 min, 23% to 35% in 8 min and climbing to 80% in 3
143 min then holding at 80% for the last 3 min, all at a constant flow rate of 400 nL/min on
144 an EASY-nLC 1000 UPLC system. The peptides were subjected to NSI source
145 followed by tandem mass spectrometry (MS/MS) in Q ExactiveTM Plus (Thermo)
146 coupled online to the UPLC. The electrospray voltage applied was 2.0 kV. The m/z
147 scan range was 350 to 1800 for full scan, and intact peptides were detected in the
148 Orbitrap at a resolution of 70,000. Peptides were then selected for MS/MS using NCE
149 setting as 28 and the fragments were detected in the Orbitrap at a resolution of 17,500.
150 A data-dependent procedure that alternated between one MS scan followed by 20
151 MS/MS scans with 15.0s dynamic exclusion. Automatic gain control (AGC) was set at

152 5E4.

153 **2.6 Database Search**

154 The resulting MS/MS data were processed using Maxquant search engine
155 (v.1.5.2.8). Tandem mass spectra were searched against *Mus musculus* data in the
156 Uniprot database concatenated with reverse decoy database. Trypsin/P was specified as
157 cleavage enzyme allowing up to 2 missing cleavages. Mass tolerance for precursor ions
158 was set as 20 ppm in First search and 5 ppm in Main search, and the mass tolerance for
159 fragment ions was set as 0.02 Da. Carbamidomethyl on Cys was specified as fixed
160 modification, oxidation on Met was specified as variable modifications. Label-free
161 quantification method was LFQ, FDR was adjusted to < 1% and the minimum score for
162 peptides was set > 40.

163 **2.7 Bioinformatic analysis**

164 Wolfsort (http://www.genscript.com/psort/wolf_psorth.html) was used to
165 predicate subcellular localization of DEPs. Eukaryotic orthologous group
166 (<http://genome.jgi.doe.gov/help/kogbrowser.jsf>) was performed on all DEPs for further
167 functional classification by aligning their sequences with the KOG database. The
168 UniProt-GOA database (<http://www.ebi.ac.uk/GOA/>) together with InterProScan soft
169 (<http://www.ebi.ac.uk/InterProScan/>) were used to analyze biological process, cellular
170 component and molecular function of DEPs. The Kyoto Encyclopedia of Genes and
171 Genomes (KEGG) database(<https://www.genome.jp/kegg>) was used to analyze
172 signaling pathways involved in DEPs. A two-tailed Fisher's exact test was employed
173 to test the enrichment of the differentially expressed protein against all identified

174 proteins. A corrected *p*-value < 0.05 was considered significant in database analysis.
175 Cluster membership was visualized by a heat map using the “heatmap.2” function from
176 the “gplots” R-package.

177 **2.8 Parallel Reaction Monitoring (PRM) Validation**

178 To verify the accuracy of Label-free proteome quantification analysis, we selected
179 18 DEPs proteins for PRM assay. The methods of protein extraction and trypsin
180 digestion were as described above. In LC-MS/MS Analysis, the gradient was comprised
181 of an increase from 6% to 23% solvent B (0.1% formic acid in 98% acetonitrile) over
182 38 min, 23% to 35% in 14 min and climbing to 80% in 4 min then holding at 80% for
183 the last 4 min, all at a constant flow rate of 700 nL/min on an EASY-nLC 1000 UPLC
184 system. Automatic gain control (AGC) was set at 3E6 for full MS and 1E5 for MS/MS.
185 The maximum IT was set at 20 ms for full MS and auto for MS/MS. The isolation
186 window for MS/MS was set at 2.0 m/z. Peptide parameters were as follows: enzyme
187 was set as Trypsin [KR/P], Max missed cleavage set as 2. The peptide length was set
188 as 8-25. precursor charges were set as 2, 3, ion charges were set as 1, 2, ion types were
189 set as b, y, p. The product ions were set as from ion 3 to last ion, the ion match tolerance
190 was set as 0.02 Da.

191 **3. Results**

192 **3.1 Identification of DEPs between C8-TA, C8-BR and C8 groups**

193 We used Label-free proteome to quantitatively analyze the host proteins and in
194 tachyzoite and tachyzoite to bradyzoite transformation stages of *T. gondii* infection
195 (Supplementary Figure 1). Among the 9 samples, a total of 32906 peptides and 30808

196 unique peptides were identified. We identified 4676 proteins as host protein, of which
197 3415 proteins were quantified (Supplementary Table S1). We defined fold change ≥ 1.5
198 or ≤ 0.67 and $p\text{-value} \leq 0.05$ as the criteria to analyze the DEPs of C8-TA, C8-BR and
199 C8 group (Figure 1A). There were a total of 163 DEPs, of which 109 were up-regulated
200 and 54 were down-regulated in C8-TA group compared with C8 group (Supplementary
201 Table S2A, Figure 1B). In addition, there were 719 DEPs, 495 host proteins were up-
202 regulated and 224 host proteins were down-regulated in C8-BR group compared with
203 C8-TA group (Supplementary Table S2B, Figure 1C).

204 **3.2 Tachyzoite infection altered multiple immunoregulatory processes in
205 astrocytes**

206 To investigate the biological functions of the DEPs between the C8-TA group and
207 the C8 group, we firstly analyzed the subcellular localization of the DEPs. As shown in
208 Figure 2A, in the C8-TA vs C8 group, 38.27% DEPs were located in cytoplasma, 14.81%
209 DEPs were located in plasma membrane, and 17.28% DEPs were located in nucleus.
210 KOG (EuKaryotic orthologous groups) was used to predict the potential functions of
211 DEPs in the C8-TA vs C8 group (Supplementary Table S3, Figure 2B). The results
212 showed that the top five KOG classifications were [U] Intracellular trafficking,
213 secretion, and vesicular transport, [J] Translation, ribosomal structure and biogenesis,
214 [O] Posttranslational modification, protein turnover, chaperones, [Z] Cytoskeleton, [A]
215 RNA processing and modification. GO enrichment analysis was performed for the
216 functional annotation of DEPs including three categories: biological process (GO-BP),
217 cellular compartment (GO-CC) and molecular function (GO-MF) (Supplementary
218 Table S4A, Figure 2C). We focused on the biological processes and found that the DEPs

219 mainly enriched in immune-related biological processes, such as defense response to
220 other organism, defense response to virus , response to interferon-beta, innate immune
221 response, detection of virus, which indicated that the DEPs mainly involved in immune
222 regulations.

223 Next, we comprehensively analyzed the biological functions of up-regulated and
224 down-regulated DEPs in C8-TA vs C8 group. The GO-BP results showed that in C8-
225 TA vs C8 group, the up-regulated DEPs were mainly involved in the following
226 biological processes: cellular hypotonic response, response to light intensity, learning,
227 ribosomal small subunit biogenesis, negative regulation of transporter activity
228 (Supplementary Table S4B, Figure 3A). The down-regulated DEPs were mainly related
229 to immune responses, such as defense response to other organisms, defense response to
230 virus, response to interferon-beta, response to virus, and innate immune response
231 (Supplementary Table S4C, Figure 3B). KEGG enrichment analysis of up-regulated
232 and down-regulated DEPs showed the signaling pathways during the infection of *T.*
233 *gondii* tachyzoites (Supplementary Table S5A, 5B). As shown in Figure 3C, D, the up-
234 regulated proteins were mapped to 18 signaling pathways, and the down-regulated
235 proteins were mapped to 10 signaling pathways in C8-TA vs C8 group. As expected
236 the down-regulated proteins were enriched in inflammatory signaling pathways, such
237 as Herpes simplex virus 1 infection , RIG-I-like receptor signaling pathway ,

238 Amoebiasis , Systemic lupus erythematosus. The above results indicated that the host
239 immune response was activated during the invasion of *T. gondii*, interestingly, our
240 results showed that the down-regulated proteins could play a major role in immune
241 regulation, which was different from the biological traits of *T. gondii* invaded epithelial

242 cells, indicated that when tachyzoites invaded astrocytes for 24 h, the immune response
243 of the host was gradually weakened. This might be a protective measurement for *T.*
244 *gondii* to avoid host astrocytes generating strong neuro-immune response.

245 **3.3 The conversion of the tachyzoites into bradyzoites upregulated glucose
246 metabolism of astrocytes**

247 Tachyzoite to bradyzoite differentiation is a key aspect of *T. gondii* biology and
248 pathogenesis. To better understand the mechanism of interaction between *T. gondii* and
249 the host during differentiation of *T. gondii*, we performed a comprehensive
250 bioinformatics analysis in C8-BR vs C8-TA group. First, we analyzed the
251 sublocalization of all DEPs by WoLF PSORT software (Figure 4A). The results showed
252 that 33% of the DEPs were localized in cytoplasm, 26% in nucleus, and 17% in
253 mitochondria. In up-regulated DEPs, most of them were located in the cytoplasm (36%),
254 followed by nucleus (21.41%) and mitochondria (20.61%) (Figure 4B). In down-
255 regulated DEPs, most of them were located in the nucleus (37%), followed by
256 cytoplasm (26%) and plasma membrane (11%) (Figure 4C).

257 We used KOG database to predict the function and classification of up and down-
258 regulated proteins (Supplementary Table S6A, 6B, Figure 4D, E). The results showed
259 that the functions of up-regulated DEPs were consistent with down-regulated DEPs,
260 and the DEPs were mainly enriched in the following categories: [O] Posttranslational
261 modification, protein turnover, chaperones, [T] Signal transduction mechanisms, [C]
262 Energy production and conversion, [U] Intracellular trafficking, secretion, and
263 vesicular transport, [A] RNA processing and modification pathway, suggested that

264 during the chronic infection stage, epigenetic mechanisms may mediate the effects on
265 host nutrient metabolism in the coexistence of host and bradyzoites. GO enrichment
266 analysis showed that the DEPs were mainly involved in metabolism-related biological
267 processes including dicarboxylic acid metabolic process, oxidoreduction coenzyme
268 metabolic process, hexose biosynthetic process, monocarboxylic acid metabolic
269 process, tricarboxylic acid metabolic process (Supplementary Table S7A,
270 Supplementary Figure 2A). Among them, glucose metabolism related biological
271 processes were up-regulated, such as dicarboxylic acid metabolic process,
272 oxidoreduction coenzyme metabolic process, carboxylic acid metabolic process,
273 tricarboxylic acid metabolic process, nucleoside phosphate metabolic process
274 (Supplementary Table S7B, Figure 5A). However, there were no significant biological
275 processes enrichment for down-regulated proteins, the top five categories of down-
276 regulated proteins were protein localization to endoplasmic reticulum, ribosomal large
277 subunit biogenesis, peptide biosynthetic process, DNA conformation change, peptide
278 metabolic process (Supplementary Table S7C, Figure 5B).

279 KEGG pathway enrichment was used to identify pathways of DEPs
280 (Supplementary Table S8A, Supplementary Figure 2B), the results showed that DEPs
281 significant enriched in metabolism-related pathways, the top five were
282 Glycolysis/Gluconeogenesis, Citrate cycle (TCA cycle), Phenylalanine metabolism,
283 Phagosome, Pyruvate metabolism. We further investigated the function of up and
284 down-regulated DEPs and found that up-regulated proteins were mainly involved in
285 metabolism-related signaling pathways including Citrate cycle (TCA cycle),

286 Glycolysis/Gluconeogenesis, Proteasome, Phagosome, Pyruvate metabolism, which
287 was consistent with the GO-BP (Supplementary Table S8B Figure 5C). The part of
288 down-regulated proteins involved in amino acid metabolism, such as Tyrosine
289 metabolism, Phenylalanine metabolism (Supplementary Table S8C, Figure 5D). During
290 the transformation from tachyzoite infection stage to bradyzoite infection stage, the
291 function of host proteins may have undergone a gradual transition from immune
292 emergency mode to up-regulation metabolic pathways. The effects on host metabolism
293 during transformation suggested that, the increased host's metabolism could accelerate
294 the decomposition of glucose, so the metabolism of *T. gondii* was decreased, which was
295 more conducive to its long-lived in their hosts.

296 **3.4 Verification of differentially expressed proteins by PRM**

297 To evaluate the accuracy of Label-free proteome quantification techniques, a total
298 of 18 DEPs were selected for PRM analysis. Based on GO and KEGG annotations, we
299 chose Bystin (Bysl), Fibronectin (Fn1), Signal transducer and activator of transcription
300 1 (Stat1), Serpin B6 (Serpib6), Guanylate-binding protein 4 (Gbp4), Interferon-
301 induced protein with tetratricopeptide repeats 3 (Ifit3), Antiviral innate immune
302 response receptor RIG-I (Ddx58), 60S ribosomal protein L23 (Rpl23), 40S ribosomal
303 protein S24 (Rps24) in C8-TA vs C8-group and Dihydrolipoyl dehydrogenase (Dld),
304 Aspartate aminotransferase, cytoplasmic (Got1), DNA (cytosine-5)-methyltransferase
305 1 (Dnmt1), Nischarin (Nisch), Enoyl-CoA hydratase, mitochondrial (Echs1),
306 Dihydrolipoyllysine-residue acetyltransferase component of pyruvate dehydrogenase
307 complex (Dlat), Tricarboxylate transport protein (Slc25a1), NAD-dependent protein

308 deacetylase sirtuin-2 (Sirt2), Omega-amidase NIT2 (Nit2) in C8-BR vs C8-TA group
309 (Figure 6, Supplementary Table S9). The results showed that the changing trends of 18
310 DEPs protein in PRM were consistent with Label-free proteome quantification,
311 suggesting that Label-free proteome quantification outcomes were relatively
312 reproducible and reliable.

313 **4. Discussion**

314 The invasion of *T. gondii* tachyzoites and bradyzoites in the host causes acute
315 infection and chronic infection respectively, resulting in clinical manifestations of
316 toxoplasma encephalopathy, chorioretinitis, miscarriage, stillbirth and
317 schizophrenia^[17,28-30]. Since there is no effective method to eliminate tissue cysts up to
318 now, the damage of host CNS caused by *T. gondii* accompany with mental and
319 behavioral disorders has been brought into focus. Therefore, understanding the
320 proteomics changes in host neuroglial cells after tachyzoites/bradyzoites infection
321 would identify the negative effects of different stages on the host, and provide targets
322 for developing new vaccines and drugs to against brain damages caused by *T. gondii*.

323 In the present study, our results showed that the DEPs in the acute infection stage
324 were mainly enriched in immune-related biological processes, while the DEPs in the
325 chronic infection stage were mainly enriched in metabolic-related biological processes.
326 Therefore our results suggested that *T. gondii* would regulate host neuroglial cells by
327 distinct mode in the two stages. Similarly, previous researches on tachyzoite infection
328 stage indicated that the up-regulated DEPs were also involved in immune inflammation
329 related pathways to prevent acute infection^[31], while those similar studies mainly based

330 on epithelial cells such as HFF cells.

331 As we know, invasion of *T. gondii* can cause inflammation in the host, and
332 astrocytes have been proved to be a pivotal regulator of CNS inflammatory responses^[32].
333 The borders and scars of astrocyte could serve as functional barriers that restrict the
334 entry of inflammatory cells into CNS parenchyma in health and disease, simultaneously,
335 it also has powerful pro-inflammatory potential. Therefore, we have established
336 acute/chronic infection models with mouse astrocytes. Interestingly, although our DEPs
337 results in tachyzoites infection models were also involved in immune inflammation
338 related pathways, changes in protein expression were very different to the results of
339 previous studies in epithelial cells.

340 In our study, the down-regulation DEPs rather than up-regulation DEPs were
341 involved in immune regulation-related processes, especially in defense response
342 pathways and innate immune response pathways. Consistently, Cekanaviciute
343 reported that after *T. gondii* infection in host CNS, the immune function must be
344 restricted to prevent excessive neuronal damage, in order to keep a balance among *T.*
345 *gondii*, brain and the immune system^[33]. As a result, we have focused on four down-
346 regulated and immune-related DEPs including Stat1, Gbp4, Ifit3 and Ddx58 after
347 tachyzoite infection. Stat1 is an important immune inflammatory factor in CNS and is
348 involved in the immune regulation of various cells. Studies have shown that inhibition
349 of Stat1 can promote bradyzoite formation^[34]. In this study, the expression of Stat1 was
350 significantly decreased, suggesting that after tachyzoite infection in astrocytes, the
351 down-regulated Stat1 might participate in promoting the transformation of tachyzoites

352 to bradyzoites, as well as inhibiting the persistent infection of tachyzoites. Gbp4 and
353 Ifit3 are IFN- γ -inducing proteins. Hu *et al* found that Gbp4 could negatively regulate
354 virus-induced type I IFN and antiviral responses by interacting with IFN regulatory
355 factor (IRF) 7 during viral infection, thus the following researches on their roles in
356 astrocytes during *T. gondii* infection may reveal a new mechanism by which astrocytes
357 against parasites^[35]. Ddx58 is also known as RIG-I, can function as an innate antiviral
358 immune response receptor and play an important role in antiviral innate immunity<sup>[36-
359 38]</sup>. In vesicular stomatitis virus (VSV)-infected astrocytes, RIG-I knockdown
360 significantly reduced inflammatory cytokine production in astrocytes^[39], and so the
361 down regulation of Ddx58 may be also involved in the transformation of tachyzoites to
362 bradyzoites in host CNS.

363 The conversation from tachyzoites to bradyzoites of *T. gondii* is a key to establish
364 chronic infection and an important link in the pathogenesis of *T. gondii*. We
365 comprehensively analyzed the DEPs between the bradyzoites infection group and the
366 tachyzoite infection group. The results showed that the DEPs were mainly involved in
367 metabolism-related biological processes and signaling pathways, and the detailed GO
368 and KEGG analyses indicated that the host's glucose metabolism and a part of amino
369 acid metabolism process have been changed significantly during chronic infection.
370 Further, we found that the up-regulated DEPs were mainly involved in glucose
371 metabolism and entered the TCA process, especially for Echs1.

372 Echs1 is a key enzyme involved in the metabolism of fatty acyl-CoA esters^[40]. In
373 fatty acid β -oxidation, it could increase the synthesis of acetyl-CoA and promoted the

374 TCA cycle, thereby increasing the process of glucose metabolism. It has been reported
375 that Echs1 deficiency (Echs1D) leaded to the impaired ATP production and metabolic
376 acidosis in patients^[41]. As an obligate intracellular parasite, *T. gondii* obtains all
377 nutrients from host cells to support its intracellular growth and proliferation. Glucose
378 and glutamine are raw materials for tachyzoites to complete the classic TCA and then
379 synthesized ATP^[42,43]. Therefore the increase of host glucose metabolism would
380 accelerate the decomposition of glucose, result in the decreasing uptake of glucose by
381 *T. gondii*. In the present study, the up-regulated Echs1 may be an important host
382 receptor of invasion parasites, and associate with the inhibition of parasites self-glucose
383 metabolism, thereby promote the formation of intracellular bradyzoites and establish
384 long-term latent infection in the host.

385 Neuronal degeneration caused by chronic infection of *T. gondii* is an important
386 pathogenesis of neurodegenerative diseases, but the mechanism has not been fully
387 elucidated. Our results also found important clues and potential targets for this process,
388 such as Dld, Sirt2 and Got1.

389 Dld, also known as Dihydrolipoyl dehydrogenase, is a mitochondrial enzyme that
390 is essential for eukaryotic cell metabolism^[44]. Ahmad reported that Dld was related to
391 Alzheimer's disease(AD), and inhibition of Dld expression would lead to a significant
392 recovery of A β pathological degradation. This could be explained that the inhibition of
393 Dld would down-regulate metabolism-related signaling pathways and reduce the host's
394 energy metabolism, which would be beneficial to alleviate the symptoms of AD^[45]. In
395 this study, we found that Dld was significantly up-regulated in bradyzoites infection

396 group, which may provide a new insight for explaining the mechanism of *T. gondii*
397 infection-induced Alzheimer's disease. In addition, Dld is also associated with severe
398 diseases in infants, causing developmental delay, hypotonia and metabolic acidosis^[46].
399 Recent studies have shown that Leishmania's self-encoded Dld induced a protective
400 cellular immune response in *L. major*-infected mice, which could serve as a design site
401 for Duchenne vaccines for kala-azar prevention^[24,47].

402 Sirt2 is an NAD⁺-dependent deacetylase that is widely involved in cell division,
403 angiogenesis^[48-50], energy metabolism^[51] and neurodegenerative^[52,53], cardiovascular
404 disease^[54,55], oxidative stress^[56] and many cancers^[57,58], etc. Studies have found that
405 Sirt2 was the most abundant sirtuin expressed in mammalian CNS, especially in cortex,
406 striatum, hippocampus, and spinal cord, suggesting that it might have a role in CNS^[59].
407 Dopaminergic (DA) neurons play a vital role in CNS, and DA neuron hyperfunction
408 was involved in several neurological disorders including schizophrenia and Parkinson's
409 Disease. Sirt2 expression was dramatically increased during the differentiation of
410 human embryonic stem cells (hESCs) into midbrain DA neurons^[60]. In addition, Sirt2
411 knockout (Sirt2^{-/-}) mice displayed fewer DA neurons and less dense striatal fibers in
412 the substantia nigra^[61]. Sirt2 inhibition also improves cognitive impairment in different
413 AD animal models and promotes neuronal survival^[62,63]. This suggested that Sirt2 can
414 be a potential therapeutic target for neurodegenerative disease. Moreover, Sirt2 is also
415 involved in ATP synthesis. Recent studies have shown that Sirt2 localized to the inner
416 mitochondrial membrane of the mouse brain, and mice lacking Sirt2 showed decreased
417 ATP levels in the striatum^[64]. In our study, the expression of Sirt2 was up-regulated

418 after chronic infection, which is consistent with Mcconkey's report, they found that
419 dopaminergic cells and brain tissues encysted with cerebral cysts have increased levels
420 of dopamine synthesis and release^[65]. Moreover, treatment of rats and mice with
421 dopamine receptor antagonists could inhibit the behavioral changes induced by *T.*
422 *gondii* infection^[66,67]. In addition, some parasites such as Leishmania, *T. brucei*, and
423 Schistosoma could encode Sirt2 homologous protein, and more importantly, it was
424 essential for parasite growth^[68-70]. Thus Sirt2 might serve as a potential treatment target
425 for psychiatric disorders induced by manipulative parasites.

426 Neuroendocrine programs and neurotransmitter imbalance may act as the
427 physiological basis for *T. gondii* induced psychiatric and behavioral disorders^[71].
428 Glutamate (GLU) is the most abundant neurotransmitter in the brain, and its excitability
429 plays a crucial role in brain structure and function. Got1 aspartate aminotransferase is
430 a type of aminotransferase that catalyzes the transamination of aspartate and α -
431 ketoglutarate to form glutamate and oxaloacetate. Glutamate dehydrogenase (Glud1) is
432 a mitochondrial enzyme that catalyzes the reductive fixation of ammonia to α -
433 ketoglutarate to form glutamate. Both Got1 and Glud1 expression were found to be up-
434 regulated in our study, suggesting that the glutamate synthesis might be increased in
435 the chronic infection group. Our finding is also consistent with a recent study, which
436 showed that chronic infection with *T. gondii* could cause an increase in extracellular
437 glutamate and a two-fold decrease in glutamate transporter expression in glial cells^[72].
438 As hyperexcitability of GLU is neurotoxic and leading to brain damage, neurological
439 disorders (eg, ALS, multiple sclerosis, AD, Huntington's disease, Parkinson's disease)

440 and psychiatric disorders (eg, schizophrenia, depression, bipolar disorder). Our finding
441 provides new evidence to explain the host mental behavioral disorders induced by
442 chronic *T. gondii* infection.

443 In conclusion, our results systematically analyzed the proteomic changes in
444 astrocytes infected with not only tachyzoites, but also bradyzoites, respectively. We
445 surprisingly discovered that *T. gondii* tachyzoites can cause down-regulation of
446 immune-related pathways in astrocytes, and the inhibited expression of Echs1 might be
447 associated with the transformation of tachyzoites to bradyzoites. However, during the
448 bradyzoites infection stage, metabolism rather than immune pathways of the host was
449 changed significantly. Both the glucose metabolism pathways and the expression of
450 some metabolism-related enzymes in astrocytes were significantly up-regulated, such
451 as Dld, Sirt2 and Got1. Since their expression was closely related to chronic
452 degenerative diseases and psychiatric diseases, which could provide a new explanation
453 for host mental and behavioral disorders induced by chronic infection of *T. gondii*.

454 **Author Contributions:** HX and KY. conceived the project and designed the
455 experiments. HX, CX, GZ, LZ, HX and LD performed the experiments. HX, KY, CX
456 analyzed the data. HS, QW, JZ and JH helped to design the layout of the pictures. HX
457 wrote the manuscript and KY revised the manuscript. All authors contributed to the
458 article and approved the submitted version.

459 **Funding:** This work was supported by Natural Science Foundation of Shandong
460 Province (ZR2022MH197), the grants from the Medicine and Health Science
461 Technology Development Plan of Shandong Province (202101050270, 202101050261),

462 Youth Science Foundation of Shandong First Medical University (Shandong Academy
463 of Medical Sciences)(202201-042), Taishan Scholars Project of Shandong Province
464 (tsqn202103186), Open research foundation of Key Laboratory for parasitic disease
465 (NHCKFKT2022-15), key research and development plan of Jining (2022YXNS152),
466 the Academic Promotion Program of Shandong First Medical University
467 (NO.2019QL005) and the Innovation Project of Shandong Academy of Medical
468 Sciences.

469 **Conflict of Interest:** The authors have no conflicts of interest to disclose.

470 **References**

- 471 1. Elmore S A, Jenkins E J, Huyvaert K P, Polley L, Root J J, Moore C G. Toxoplasma
472 gondii in circumpolar people and wildlife. *Vector borne and zoonotic diseases*
473 (Larchmont, NY). 2012; 12(1):1-9. 10.1089/vbz.2011.0705
- 474 2. Chen J, Xu M J, Zhou D H, Song H Q, Wang C R, Zhu X Q. Canine and feline
475 parasitic zoonoses in China. *Parasit Vectors*. 2012; 5:152. 10.1186/1756-3305-5-
476 152
- 477 3. Boughattas S, Bergaoui R, Essid R, Aoun K, Bourabtine A. Seroprevalence of
478 Toxoplasma gondii infection among horses in Tunisia. *Parasit Vectors*. 2011; 4:218.
479 10.1186/1756-3305-4-218
- 480 4. Montoya J G, Liesenfeld O. Toxoplasmosis. *Lancet* (London, England). 2004;
481 363(9425):1965-1976. 10.1016/s0140-6736(04)16412-x
- 482 5. Tenter A M, Heckeroth A R, Weiss L M. Toxoplasma gondii: from animals to
483 humans. *International journal for parasitology*. 2000; 30(12-13):1217-1258.
484 10.1016/s0020-7519(00)00124-7
- 485 6. Dong H, Su R, Lu Y, Wang M, Liu J, Jian F, et al. Prevalence, Risk Factors, and
486 Genotypes of Toxoplasma gondii in Food Animals and Humans (2000-2017) From
487 China. *Frontiers in microbiology*. 2018; 9:2108. 10.3389/fmicb.2018.02108
- 488 7. Luft B J, Remington J S. Toxoplasmic encephalitis. *Journal of Infectious Diseases*.
489 1988; 157(1):1-6. 10.1093/infdis/157.1.1
- 490 8. Antinori A, Larussa D, Cingolani A, Lorenzini P, Bossolasco S, Finazzi M G, et al.
491 Prevalence, associated factors, and prognostic determinants of AIDS-related
492 toxoplasmic encephalitis in the era of advanced highly active antiretroviral therapy.
493 *Clinical infectious diseases : an official publication of the Infectious Diseases*
494 *Society of America*. 2004; 39(11):1681-1691. 10.1086/424877
- 495 9. Mohraz M, Mehrkhani F, Jam S, Seyedalinaghi S, Sabzvari D, Fattahi F, et al.

496 Seroprevalence of toxoplasmosis in HIV(+)/AIDS patients in Iran. *Acta medica*
497 *Iranica*. 2011; 49(4):213-218. 21713730

498 10. Watts E, Zhao Y, Dhara A, Eller B, Patwardhan A, Sinai A P. Novel Approaches
499 Reveal that *Toxoplasma gondii* Bradyzoites within Tissue Cysts Are Dynamic and
500 Replicating Entities In Vivo. *mBio*. 2015; 6(5):e01155-01115.
501 10.1128/mBio.01155-15

502 11. Quatrini L, Vivier E, Ugolini S. Neuroendocrine regulation of innate lymphoid cells.
503 *Immunological reviews*. 2018; 286(1):120-136. 10.1111/imr.12707

504 12. Xiao J, Savonenko A, Yolken R H. Strain-specific pre-existing immunity: A key to
505 understanding the role of chronic *Toxoplasma* infection in cognition and
506 Alzheimer's diseases? *Neuroscience and biobehavioral reviews*. 2022; 137:104660.
507 10.1016/j.neubiorev.2022.104660

508 13. Stock A K, Heintschel Von Heinegg E, Köhling H L, Beste C. Latent *Toxoplasma*
509 *gondii* infection leads to improved action control. *Brain, behavior, and immunity*.
510 2014; 37:103-108. 10.1016/j.bbi.2013.11.004

511 14. Flegl J. How and why *Toxoplasma* makes us crazy. *Trends in parasitology*. 2013;
512 29(4):156-163. 10.1016/j.pt.2013.01.007

513 15. Vyas A, Kim S K, Giacomini N, Boothroyd J C, Sapsky R M. Behavioral changes
514 induced by *Toxoplasma* infection of rodents are highly specific to aversion of cat
515 odors. *Proceedings of the National Academy of Sciences of the United States of*
516 *America*. 2007; 104(15):6442-6447. 10.1073/pnas.0608310104

517 16. Boillat M, Hammoudi P M, Dogga S K, Pagès S, Goubran M, Rodriguez I, et al.
518 Neuroinflammation-Associated Aspecific Manipulation of Mouse Predator Fear by
519 *Toxoplasma gondii*. *Cell reports*. 2020; 30(2):320-334.e326.
520 10.1016/j.celrep.2019.12.019

521 17. Hamidinejat H, Ghorbanpoor M, Hosseini H, Alavi S M, Nabavi L, Jalali M H, et
522 al. *Toxoplasma gondii* infection in first-episode and inpatient individuals with
523 schizophrenia. *International journal of infectious diseases : IJID : official*
524 *publication of the International Society for Infectious Diseases*. 2010; 14(11):e978-
525 981. 10.1016/j.ijid.2010.05.018

526 18. Ansari-Lari M, Farashbandi H, Mohammadi F. Association of *Toxoplasma gondii*
527 infection with schizophrenia and its relationship with suicide attempts in these
528 patients. *Tropical medicine & international health : TM & IH*. 2017; 22(10):1322-
529 1327. 10.1111/tmi.12933

530 19. Oncu-Oner T, Can S. Meta-analysis of the relationship between *Toxoplasma gondii*
531 and schizophrenia. *Annals of parasitology*. 2022; 68(1):103-110.
532 10.17420/ap6801.414

533 20. Sutterland A L, Kuin A, Kuiper B, Van Gool T, Leboyer M, Fond G, et al. Driving
534 us mad: the association of *Toxoplasma gondii* with suicide attempts and traffic
535 accidents - a systematic review and meta-analysis. *Psychological medicine*. 2019;
536 49(10):1608-1623. 10.1017/s0033291719000813

537 21. Halonen S K, Lyman W D, Chiu F C. Growth and development of *Toxoplasma*
538 *gondii* in human neurons and astrocytes. *Journal of neuropathology and*

539 experimental neurology. 1996; 55(11):1150-1156. 10.1097/00005072-199611000-
540 00006

541 22. Eroglu C, Barres B A. Regulation of synaptic connectivity by glia. *Nature*. 2010;
542 468(7321):223-231. 10.1038/nature09612

543 23. Morita M, Ikeshima-Kataoka H, Kreft M, Vardjan N, Zorec R, Noda M. Metabolic
544 Plasticity of Astrocytes and Aging of the Brain. *International journal of molecular
545 sciences*. 2019; 20(4):10.3390/ijms20040941

546 24. Daneman R, Prat A. The blood-brain barrier. *Cold Spring Harbor perspectives in
547 biology*. 2015; 7(1):a020412. 10.1101/csphperspect.a020412

548 25. Allen N J, Eroglu C. Cell Biology of Astrocyte-Synapse Interactions. *Neuron*. 2017;
549 96(3):697-708. 10.1016/j.neuron.2017.09.056

550 26. Perez-Catalan N A, Doe C Q, Ackerman S D. The role of astrocyte-mediated
551 plasticity in neural circuit development and function. *Neural development*. 2021;
552 16(1):1. 10.1186/s13064-020-00151-9

553 27. Blanchard N, Dunay I R, Schlüter D. Persistence of *Toxoplasma gondii* in the
554 central nervous system: a fine-tuned balance between the parasite, the brain and the
555 immune system. *Parasite immunology*. 2015; 37(3):150-158. 10.1111/pim.12173

556 28. Caselli D, Andreoli E, Paolicchi O, Savelli S, Guidi S, Pecile P, et al. Acute
557 encephalopathy in the immune-compromised child: never forget toxoplasmosis.
558 *Journal of pediatric hematology/oncology*. 2012; 34(5):383-386.
559 10.1097/MPH.0b013e318257a15c

560 29. Montoya J G, Remington J S. Toxoplasmic chorioretinitis in the setting of acute
561 acquired toxoplasmosis. *Clinical infectious diseases : an official publication of the
562 Infectious Diseases Society of America*. 1996; 23(2):277-282.
563 10.1093/clinids/23.2.277

564 30. Alvarado-Esquível C, Pacheco-Vega S J, Hernández-Tinoco J, Centeno-Tinoco M
565 M, Beristain-García I, Sánchez-Anguiano L F, et al. Miscarriage history and
566 *Toxoplasma gondii* infection: A cross-sectional study in women in Durango City,
567 Mexico. *European journal of microbiology & immunology*. 2014; 4(2):117-122.
568 10.1556/EuJMI.4.2014.2.4

569 31. Sun H, Li J, Wang L, Yin K, Xu C, Liu G, et al. Comparative Proteomics Analysis
570 for Elucidating the Interaction Between Host Cells and *Toxoplasma gondii*.
571 *Frontiers in cellular and infection microbiology*. 2021; 11:643001.
572 10.3389/fcimb.2021.643001

573 32. Sofroniew M V. Astrocyte barriers to neurotoxic inflammation. *Nature reviews
574 Neuroscience*. 2015; 16(5):249-263. 10.1038/nrn3898

575 33. Cekanaviciute E, Dietrich H K, Axtell R C, Williams A M, Egusquiza R, Wai K M,
576 et al. Astrocytic TGF- β signaling limits inflammation and reduces neuronal damage
577 during central nervous system *Toxoplasma* infection. *Journal of immunology
(Baltimore, Md : 1950)*. 2014; 193(1):139-149. 10.4049/jimmunol.1303284

578 34. Hidano S, Randall L M, Dawson L, Dietrich H K, Konradt C, Klover P J, et al.
579 STAT1 Signaling in Astrocytes Is Essential for Control of Infection in the Central
580 Nervous System. *mBio*. 2016; 7(6): e01881-16.10.1128/mBio.01881-16
581

582 35. Hu Y, Wang J, Yang B, Zheng N, Qin M, Ji Y, et al. Guanylate binding protein 4
583 negatively regulates virus-induced type I IFN and antiviral response by targeting
584 IFN regulatory factor 7. *Journal of immunology* (Baltimore, Md : 1950). 2011;
585 187(12):6456-6462. 10.4049/jimmunol.1003691

586 36. Yoneyama M, Fujita T. Function of RIG-I-like receptors in antiviral innate
587 immunity. *The Journal of biological chemistry*. 2007; 282(21):15315-15318.
588 10.1074/jbc.R700007200

589 37. Yoneyama M, Kikuchi M, Natsukawa T, Shinobu N, Imaizumi T, Miyagishi M, et
590 al. The RNA helicase RIG-I has an essential function in double-stranded RNA-
591 induced innate antiviral responses. *Nature immunology*. 2004; 5(7):730-737.
592 10.1038/ni1087

593 38. Kato H, Sato S, Yoneyama M, Yamamoto M, Uematsu S, Matsui K, et al. Cell type-
594 specific involvement of RIG-I in antiviral response. *Immunity*. 2005; 23(1):19-28.
595 10.1016/j.jimmuni.2005.04.010

596 39. Furr S R, Moerdyk-Schauwecker M, Grdzelishvili V Z, Marriott I. RIG-I mediates
597 nonsegmented negative-sense RNA virus-induced inflammatory immune responses
598 of primary human astrocytes. *Glia*. 2010; 58(13):1620-1629. 10.1002/glia.21034

599 40. Finsterer J. Metabolische Myopathien–Teil I: Störungen des
600 Kohlehydratstoffwechsels. *Fortschritte der Neurologie- Psychiatrie*. 2011;
601 79(10):598-606. 10.1002/glia.21034

602 41. Brown G K, Hunt S M, Scholem R, Fowler K, Grimes A, Mercer J F, et al. beta-
603 hydroxyisobutyryl coenzyme A deacylase deficiency: a defect in valine metabolism
604 associated with physical malformations. *Pediatrics*. 1982; 70(4):532-538. 7122152

605 42. Blume M, Rodriguez-Contreras D, Landfear S, Fleige T, Soldati-Favre D, Lucius
606 R, et al. Host-derived glucose and its transporter in the obligate intracellular
607 pathogen *Toxoplasma gondii* are dispensable by glutaminolysis. *Proceedings of the
608 National Academy of Sciences of the United States of America*. 2009;
609 106(31):12998-13003. 10.1073/pnas.0903831106

610 43. Macrae J I, Sheiner L, Nahid A, Tonkin C, Striepen B, Mcconville M J.
611 Mitochondrial metabolism of glucose and glutamine is required for intracellular
612 growth of *Toxoplasma gondii*. *Cell host & microbe*. 2012; 12(5):682-692.
613 10.1016/j.chom.2012.09.013

614 44. Babady N E, Pang Y P, Elpeleg O, Isaya G. Cryptic proteolytic activity of
615 dihydrolipoamide dehydrogenase. *Proceedings of the National Academy of
616 Sciences of the United States of America*. 2007; 104(15):6158-6163.
617 10.1073/pnas.0610618104

618 45. Ahmad W, Ebert P R. Suppression of a core metabolic enzyme dihydrolipoamide
619 dehydrogenase (dld) protects against amyloid beta toxicity in *C. elegans* model of
620 Alzheimer's disease. *Genes & diseases*. 2021; 8(6):849-866.
621 10.1016/j.gendis.2020.08.004

622 46. Ambrus A, Adam-Vizi V. Human dihydrolipoamide dehydrogenase (E3) deficiency:
623 Novel insights into the structural basis and molecular pathomechanism.
624 *Neurochemistry international*. 2018; 117:5-14. 10.1016/j.neuint.2017.05.018

625 47. Mou Z, Barazandeh A F, Hamana H, Kishi H, Zhang X, Jia P, et al. Identification
626 of a Protective Leishmania Antigen Dihydrolipoyl Dehydrogenase and Its
627 Responding CD4(+) T Cells at Clonal Level. *Journal of immunology* (Baltimore,
628 Md : 1950). 2020; 205(5):1355-1364. 10.4049/jimmunol.2000338

629 48. Voelter-Mahlknecht S, Ho A D, Mahlknecht U. FISH-mapping and genomic
630 organization of the NAD-dependent histone deacetylase gene, Sirtuin 2 (Sirt2).
631 *International journal of oncology*. 2005; 27(5):1187-1196. 10.3892/ijo.27.5.1187

632 49. Li C, Zhou Y, Rychahou P, Weiss H L, Lee E Y, Perry C L, et al. SIRT2 Contributes
633 to the Regulation of Intestinal Cell Proliferation and Differentiation. *Cellular and*
634 *molecular gastroenterology and hepatology*. 2020; 10(1):43-57.
635 10.1016/j.jcmgh.2020.01.004

636 50. Hu F, Sun X, Li G, Wu Q, Chen Y, Yang X, et al. Inhibition of SIRT2 limits tumour
637 angiogenesis via inactivation of the STAT3/VEGFA signalling pathway. *Cell death*
638 & disease. 2018; 10(1):9. 10.1038/s41419-018-1260-z

639 51. Park S, Chung M J, Son J Y, Yun H H, Park J M, Yim J H, et al. The role of Sirtuin
640 2 in sustaining functional integrity of the liver. *Life sciences*. 2021; 285:119997.
641 10.1016/j.lfs.2021.119997

642 52. Zhang Y, Anoopkumar-Dukie S, Arora D, Davey A K. Review of the anti-
643 inflammatory effect of SIRT1 and SIRT2 modulators on neurodegenerative diseases.
644 *European journal of pharmacology*. 2020; 867:172847.
645 10.1016/j.ejphar.2019.172847

646 53. Manjula R, Anuja K, Alcain F J. SIRT1 and SIRT2 Activity Control in
647 Neurodegenerative Diseases. *Frontiers in pharmacology*. 2020; 11:585821.
648 10.3389/fphar.2020.585821

649 54. Zhang N, Zhang Y, Wu B, Wu S, You S, Lu S, et al. Deacetylation-dependent
650 regulation of PARP1 by SIRT2 dictates ubiquitination of PARP1 in oxidative stress-
651 induced vascular injury. *Redox biology*. 2021; 47:102141.
652 10.1016/j.redox.2021.102141

653 55. Wu B, You S, Qian H, Wu S, Lu S, Zhang Y, et al. The role of SIRT2 in vascular-
654 related and heart-related diseases: A review. *Journal of cellular and molecular*
655 *medicine*. 2021; 25(14):6470-6478. 10.1111/jcmm.16618

656 56. Yang M, Peng Y, Liu W, Zhou M, Meng Q, Yuan C. Sirtuin 2 expression suppresses
657 oxidative stress and senescence of nucleus pulposus cells through inhibition of the
658 p53/p21 pathway. *Biochemical and biophysical research communications*. 2019;
659 513(3):616-622. 10.1016/j.bbrc.2019.03.200

660 57. Farooqi A S, Hong J Y, Cao J, Lu X, Price I R, Zhao Q, et al. Novel Lysine-Based
661 Thioureas as Mechanism-Based Inhibitors of Sirtuin 2 (SIRT2) with Anticancer
662 Activity in a Colorectal Cancer Murine Model. *Journal of medicinal chemistry*.
663 2019; 62(8):4131-4141. 10.1021/acs.jmedchem.9b00191

664 58. Zhao N, Guo Y, Liu P, Chen Y, Wang Y. Sirtuin 2 promotes cell stemness and
665 MEK/ERK signaling pathway while reduces chemosensitivity in endometrial
666 cancer. *Archives of gynecology and obstetrics*. 2022; 305(3):693-701.
667 10.1007/s00404-021-06216-2

668 59. Maxwell M M, Tomkinson E M, Nobles J, Wizeman J W, Amore A M, Quinti L, et
669 al. The Sirtuin 2 microtubule deacetylase is an abundant neuronal protein that
670 accumulates in the aging CNS. *Human molecular genetics*. 2011; 20(20):3986-3996.
671 10.1093/hmg/ddr326

672 60. Cha Y, Han M J, Cha H J, Zoldan J, Burkart A, Jung J H, et al. Metabolic control
673 of primed human pluripotent stem cell fate and function by the miR-200c-SIRT2
674 axis. *Nature cell biology*. 2017; 19(5):445-456. 10.1038/ncb3517

675 61. Szegő É M, Gerhardt E, Outeiro T F. Sirtuin 2 enhances dopaminergic
676 differentiation via the AKT/GSK-3 β /β-catenin pathway. *Neurobiology of aging*.
677 2017; 56:7-16. 10.1016/j.neurobiolaging.2017.04.001

678 62. Biella G, Fusco F, Nardo E, Bernocchi O, Colombo A, Lichtenthaler S F, et al.
679 Sirtuin 2 Inhibition Improves Cognitive Performance and Acts on Amyloid- β
680 Protein Precursor Processing in Two Alzheimer's Disease Mouse Models. *Journal
681 of Alzheimer's disease : JAD*. 2016; 53(3):1193-1207. 10.3233/jad-151135

682 63. Wang Y, Yang J Q, Hong T T, Sun Y H, Huang H L, Chen F, et al. RTN4B-
683 mediated suppression of Sirtuin 2 activity ameliorates β -amyloid pathology and
684 cognitive impairment in Alzheimer's disease mouse model. *Aging cell*. 2020;
685 19(8):e13194. 10.1111/ace.13194

686 64. Liu G, Park S H, Imbesi M, Nathan W J, Zou X, Zhu Y, et al. Loss of NAD-
687 Dependent Protein Deacetylase Sirtuin-2 Alters Mitochondrial Protein Acetylation
688 and Dysregulates Mitophagy. *Antioxidants & redox signaling*. 2017; 26(15):849-
689 863. 10.1089/ars.2016.6662

690 65. Mcconkey G A, Martin H L, Bristow G C, Webster J P. *Toxoplasma gondii*
691 infection and behaviour - location, location, location? *The Journal of experimental
692 biology*. 2013; 216(Pt 1):113-119. 10.1242/jeb.074153

693 66. Webster J P, Lamberton P H, Donnelly C A, Torrey E F. Parasites as causative
694 agents of human affective disorders? The impact of anti-psychotic, mood-stabilizer
695 and anti-parasite medication on *Toxoplasma gondii*'s ability to alter host behaviour.
696 *Proceedings Biological sciences*. 2006; 273(1589):1023-1030.
697 10.1098/rspb.2005.3413

698 67. Skallová A, Kodym P, Frynta D, Flegr J. The role of dopamine in *Toxoplasma*-
699 induced behavioural alterations in mice: an ethological and ethopharmacological
700 study. *Parasitology*. 2006; 133(Pt 5):525-535. 10.1017/s0031182006000886

701 68. Roiko M S, Lafavers K, Leland D, Arrizabalaga G. *Toxoplasma gondii*-positive
702 human sera recognise intracellular tachyzoites and bradyzoites with diverse patterns
703 of immunoreactivity. *International journal for parasitology*. 2018; 48(3-4):225-232.
704 10.1016/j.ijpara.2017.08.016

705 69. Ronin C, Costa D M, Tavares J, Faria J, Ciesielski F, Ciapetti P, et al. The crystal
706 structure of the *Leishmania infantum* Silent Information Regulator 2 related protein
707 1: Implications to protein function and drug design. *PloS one*. 2018; 13(3):e0193602.
708 10.1371/journal.pone.0193602

709 70. García-Salcedo J A, Gijón P, Nolan D P, Tebabi P, Pays E. A chromosomal SIR2
710 homologue with both histone NAD-dependent ADP-ribosyltransferase and

711 deacetylase activities is involved in DNA repair in *Trypanosoma brucei*. The EMBO
712 journal. 2003; 22(21):5851-5862. 10.1093/emboj/cdg553

713 71. Yin K, Xu C, Zhao G, Xie H. Epigenetic Manipulation of Psychiatric Behavioral
714 Disorders Induced by *Toxoplasma gondii*. Frontiers in cellular and infection
715 microbiology. 2022; 12:803502. 10.3389/fcimb.2022.803502

716 72. David C N, Frias E S, Szu J I, Vieira P A, Hubbard J A, Lovelace J, et al. GLT-1-
717 Dependent Disruption of CNS Glutamate Homeostasis and Neuronal Function by
718 the Protozoan Parasite *Toxoplasma gondii*. PLoS pathogens. 2016; 12(6):e1005643.
719 10.1371/journal.ppat.1005643

720

721

722 **Figure legends:**

723 **Figure 1 Proteome analysis of DEPs in tachyzoite and tachyzoite to bradyzoite**
724 **transformation stages of *T. gondii* infection.** (A) Heat map shown the DEPs in the
725 three groups. (B) Volcano plot shown DEPs between the C8-TA group and the C8
726 group. (C) Volcano plot shown DEPs between the C8-BR group and the C8 group.

727 **Figure 2 Location and functional classification of DEPs between the C8-TA group**
728 **and the C8 group.** (A) Location of subcellular structures of DEPs between the C8-TA
729 group and the C8 group. (B) KOG classification of DEPs between the C8-TA group
730 and the C8 group. (C) GO enrichment analysis of DEPs between C8-TA vs C8 group
731 included biological process, cellular composition, and biological function.

732 **Figure 3 GO and KEGG pathway enrichment analysis of up-regulated and down-**
733 **regulated DEPs between C8-TA group and C8 groups.** (A) GO enrichment analysis
734 of up-regulated DEPs. (B) GO enrichment analysis of down-regulated DEPs. (C)
735 KEGG pathway enrichment analysis of up-regulated DEPs. (D) KEGG pathway
736 enrichment analysis of down-regulated DEPs.

737 **Figure 4 Subcellular localization and functional classification of DEPs between**
738 **C8-BR group and C8-TA groups.** (A) The location of subcellular structures of all
739 DEPs. (B) The location of subcellular structures of up-regulated DEPs. (C) The location
740 of subcellular structures of down-regulated DEPs. (D) The KOG classification of up-
741 regulated DEPs. (E) The KOG classification of down-regulated DEPs.

742 **Figure 5 GO and KEGG pathway enrichment analysis of up-regulated and down-**
743 **regulated DEPs between C8-BR group and C8-RH groups.** (A) GO enrichment

744 analysis of up-regulated DEPs. (B) GO enrichment analysis of down-regulated DEPs.
745 (C) KEGG pathway enrichment analysis of up-regulated DEPs. (D) KEGG pathway
746 enrichment analysis of down-regulated DEPs.

747 **Figure 6 Comparative analyses of label-free proteomics and PRM results for 18**
748 **screened DEPs.**

749 **Supplementary Figure 1 Agarose gel electrophoresis of PCR product for BAG1**
750 **gene.**

751 **Supplementary Figure 2 GO and KEGG enrichment analysis of all DEPs between**
752 **C8-BR group and C8-RH group.** (A) GO enrichment analysis of all DEPs. (B) KEGG
753 enrichment analysis of all DEP.

A

bioRxiv preprint doi: <https://doi.org/10.1101/2023.01.15.524169>; this version posted January 19, 2023. The copyright holder for this preprint (which was not certified by peer review) is the author/funder, who has granted bioRxiv a license to display the preprint in perpetuity. It is made available under aCC-BY 4.0 International license.

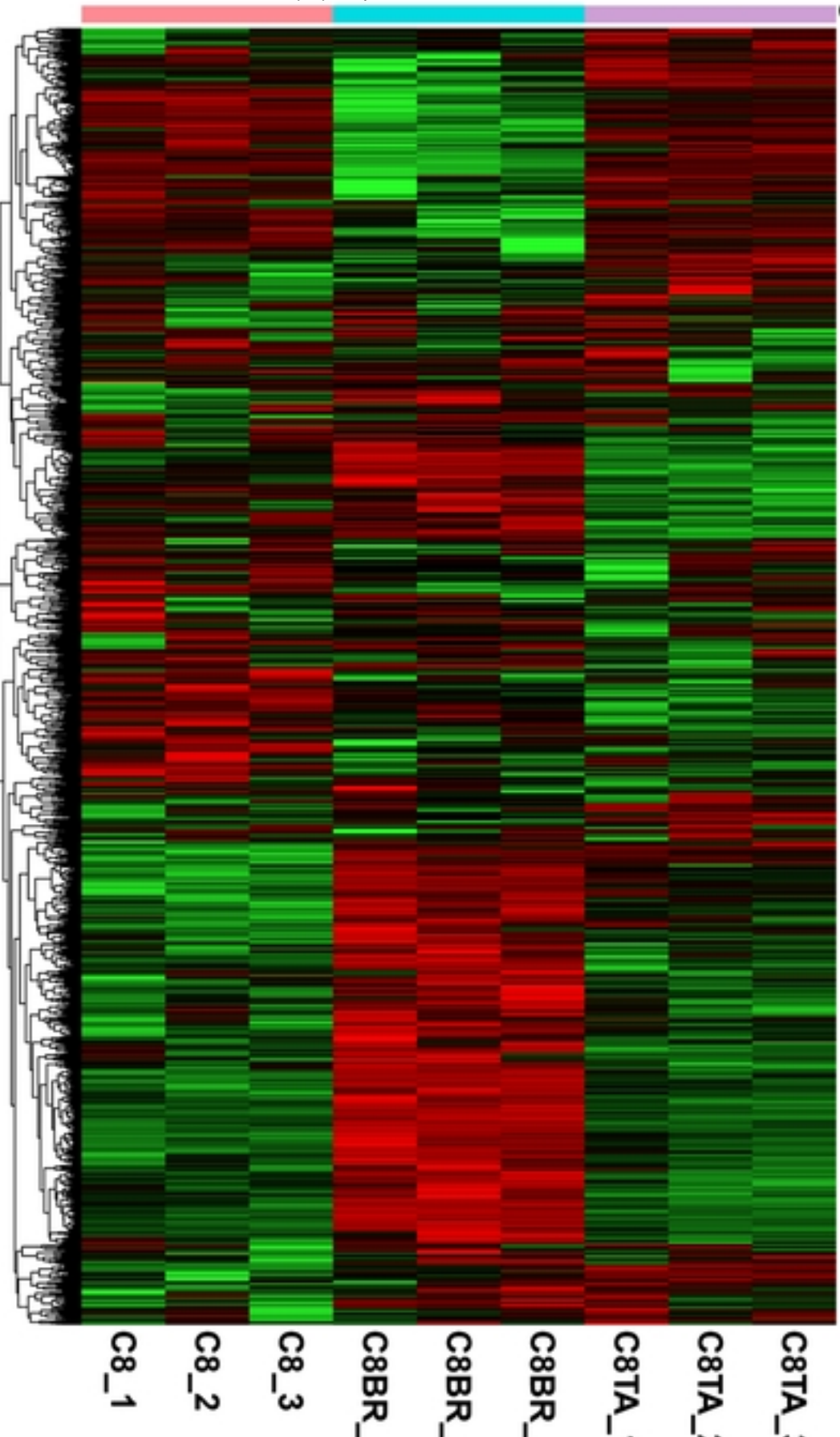
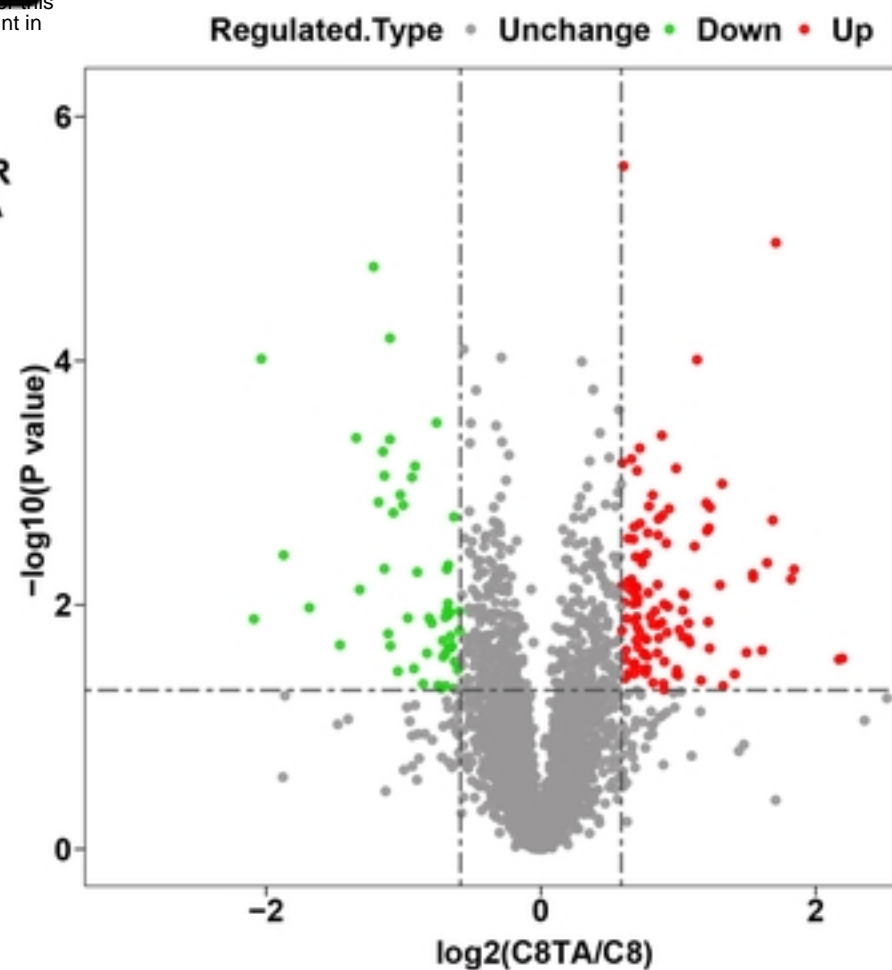
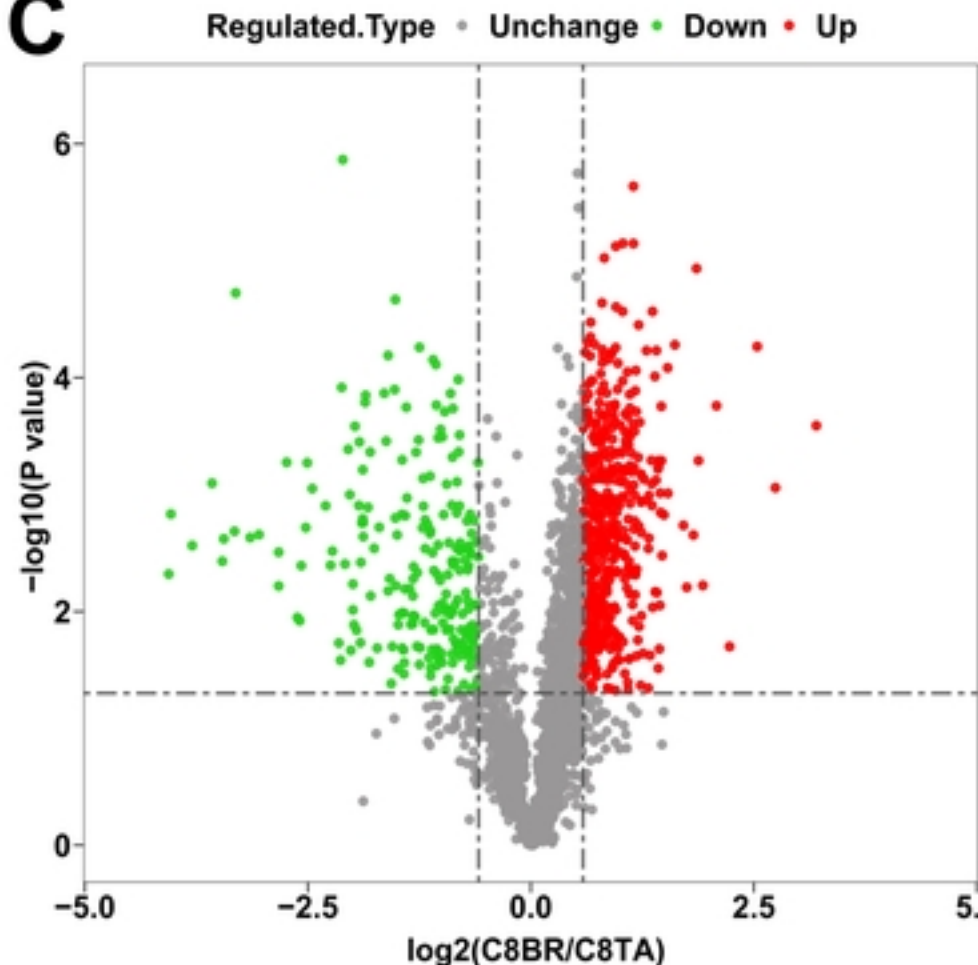
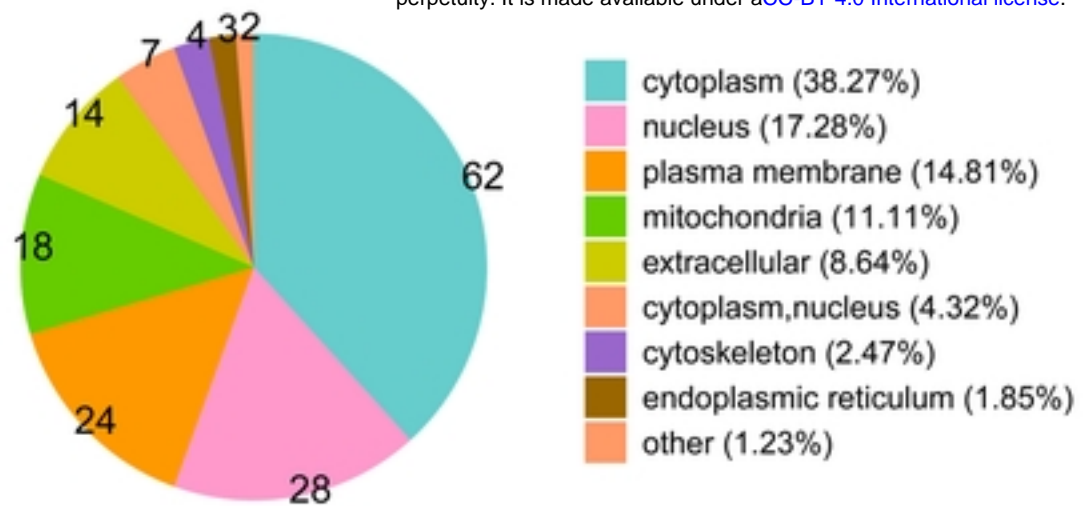
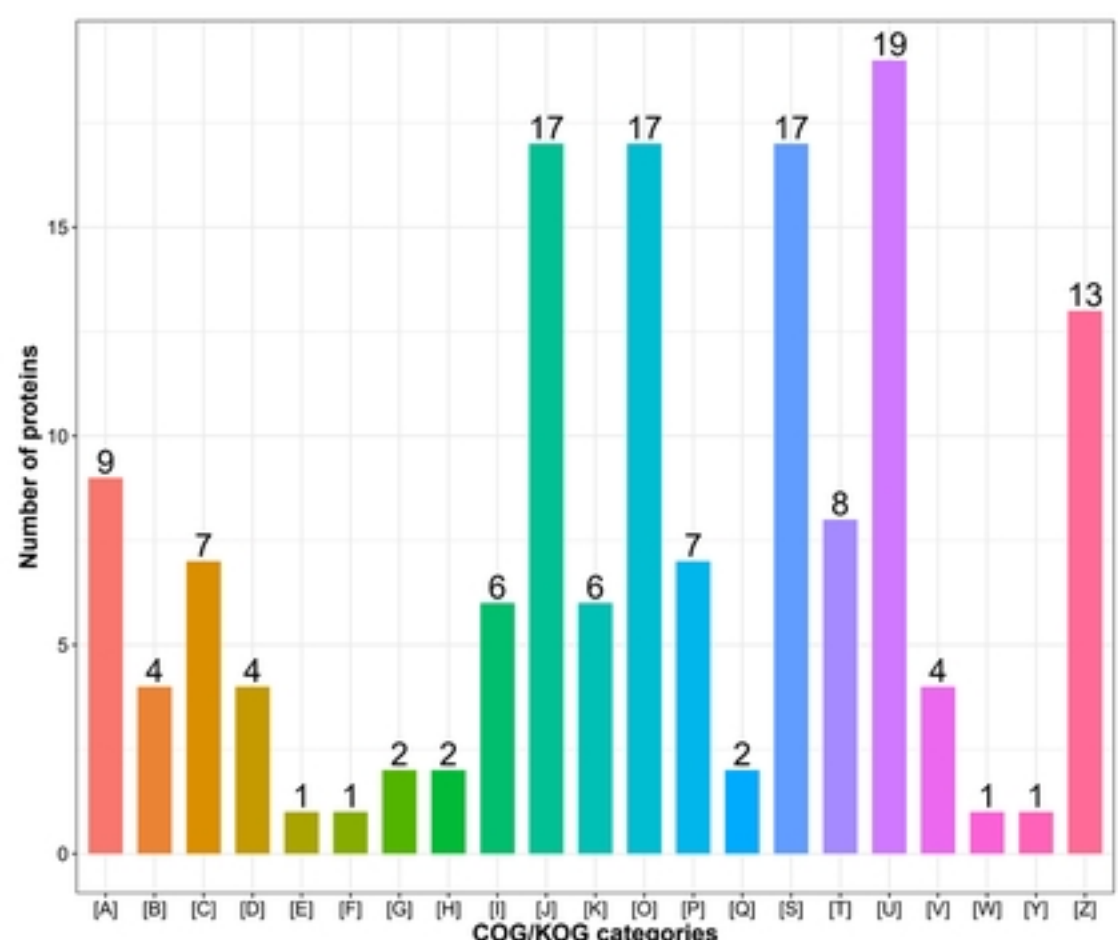
**B****C**

Figure1

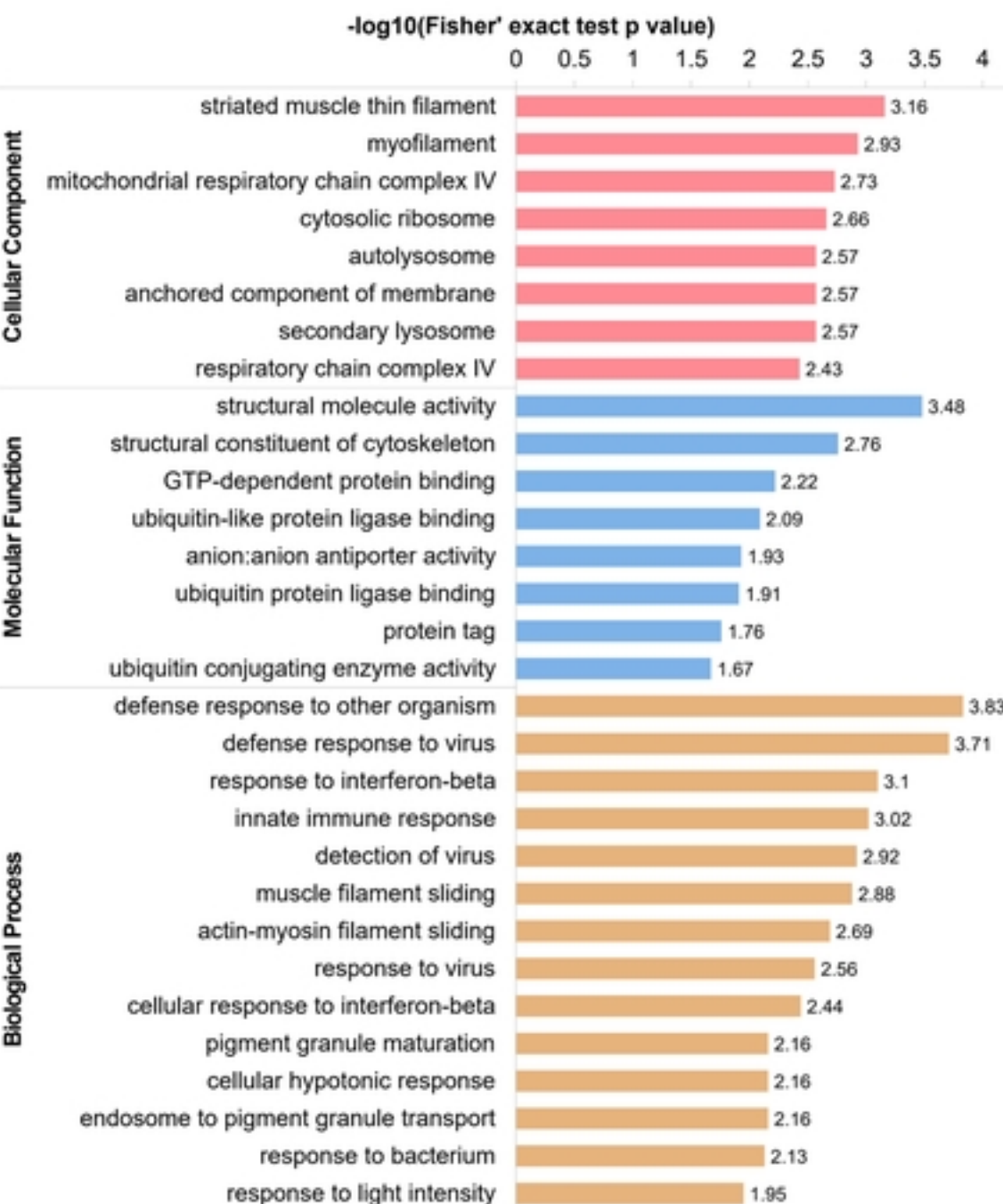
A

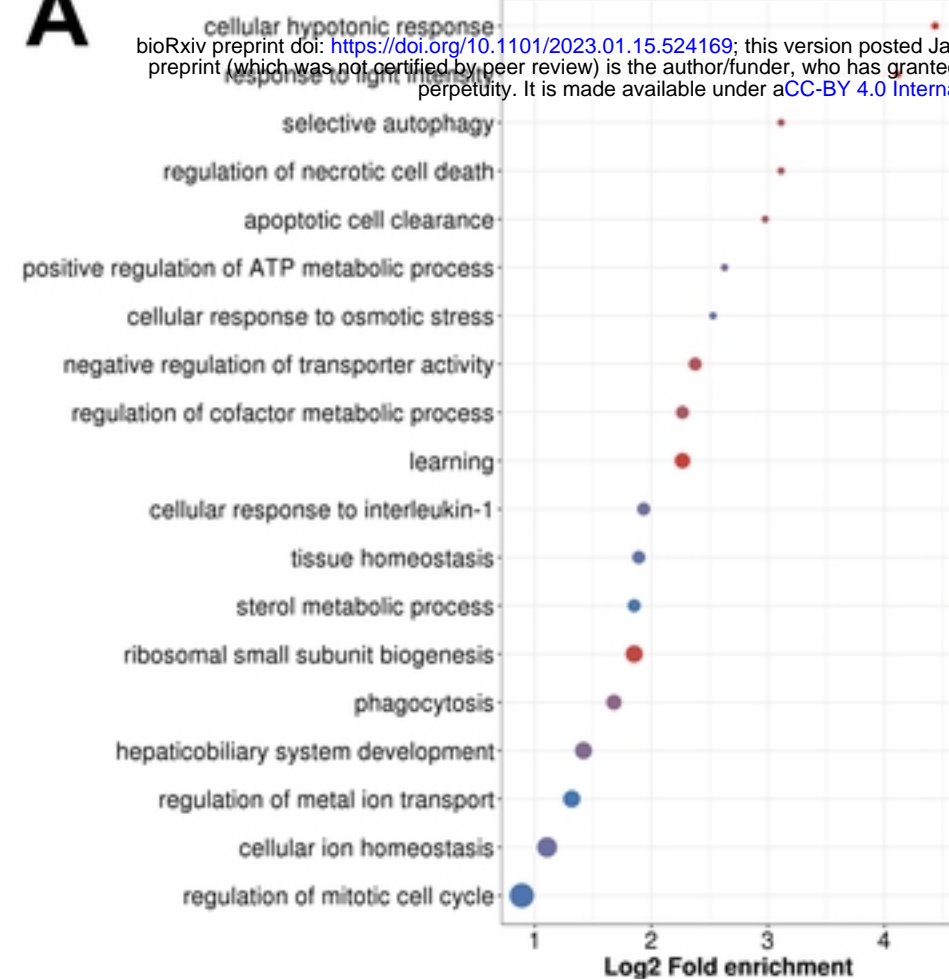
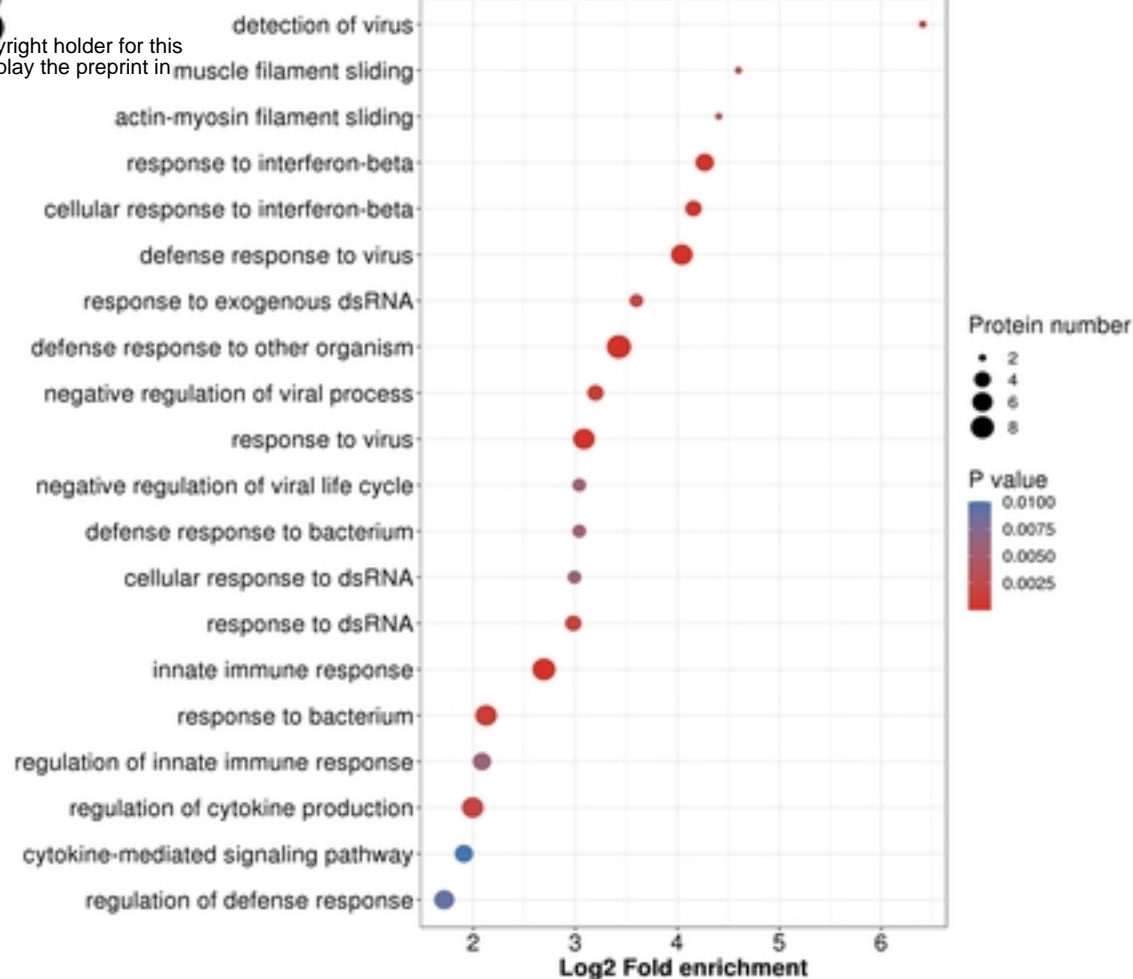
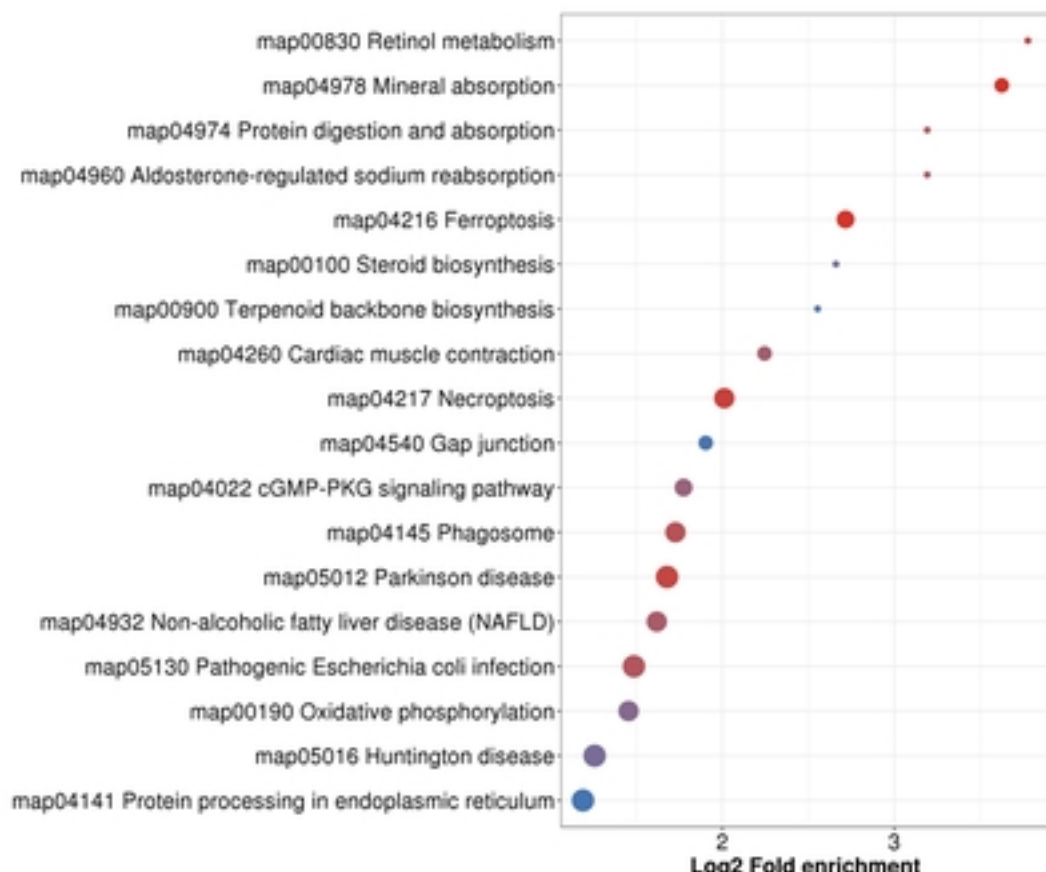
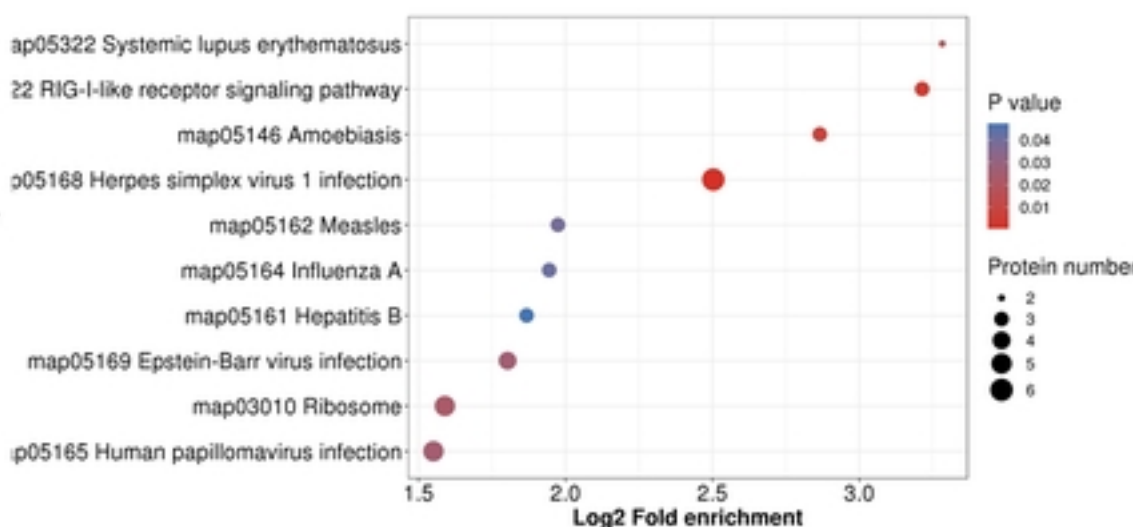
bioRxiv preprint doi: <https://doi.org/10.1101/2023.01.15.524169>; this version posted January 19, 2023. The copyright holder for this preprint (which was not certified by peer review) is the author/funder, who has granted bioRxiv a license to display the preprint in perpetuity. It is made available under aCC-BY 4.0 International license.

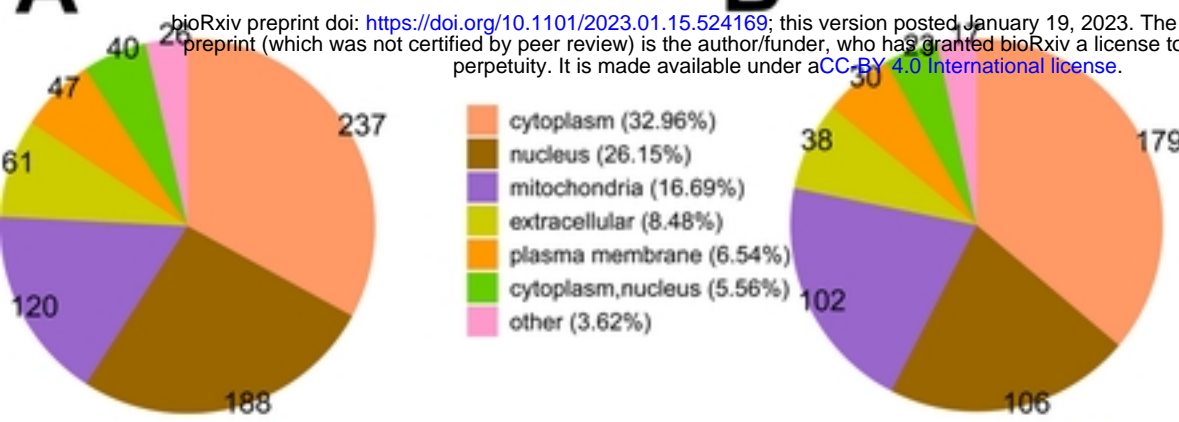
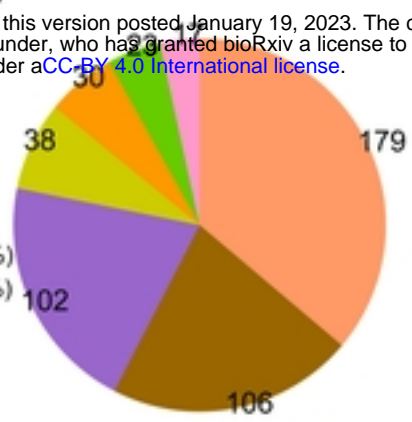
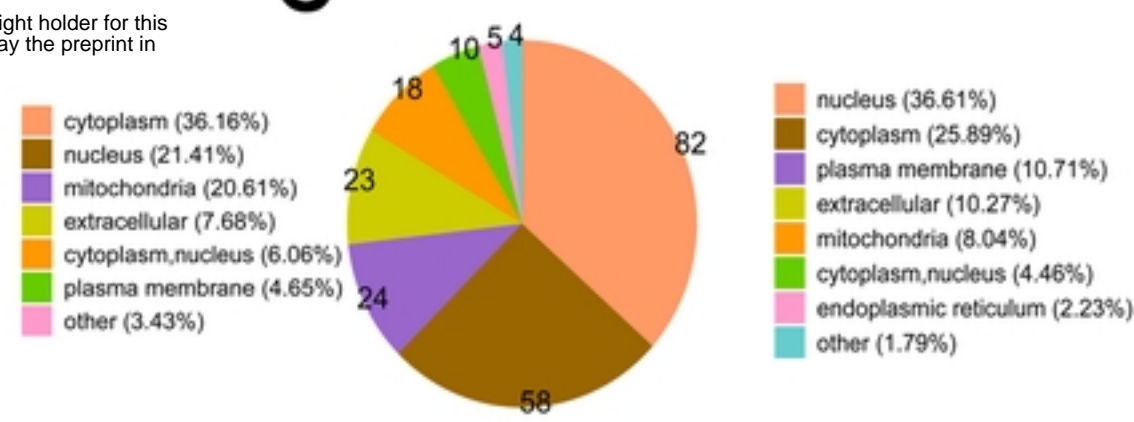
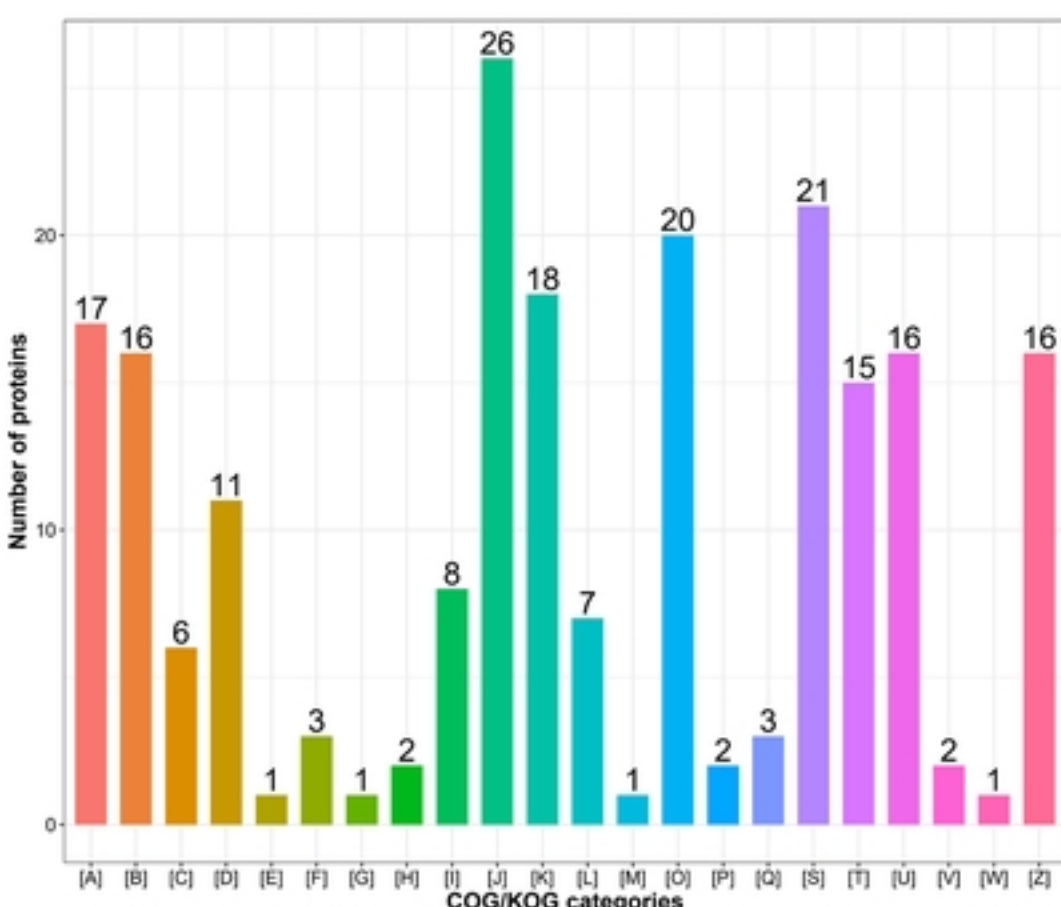
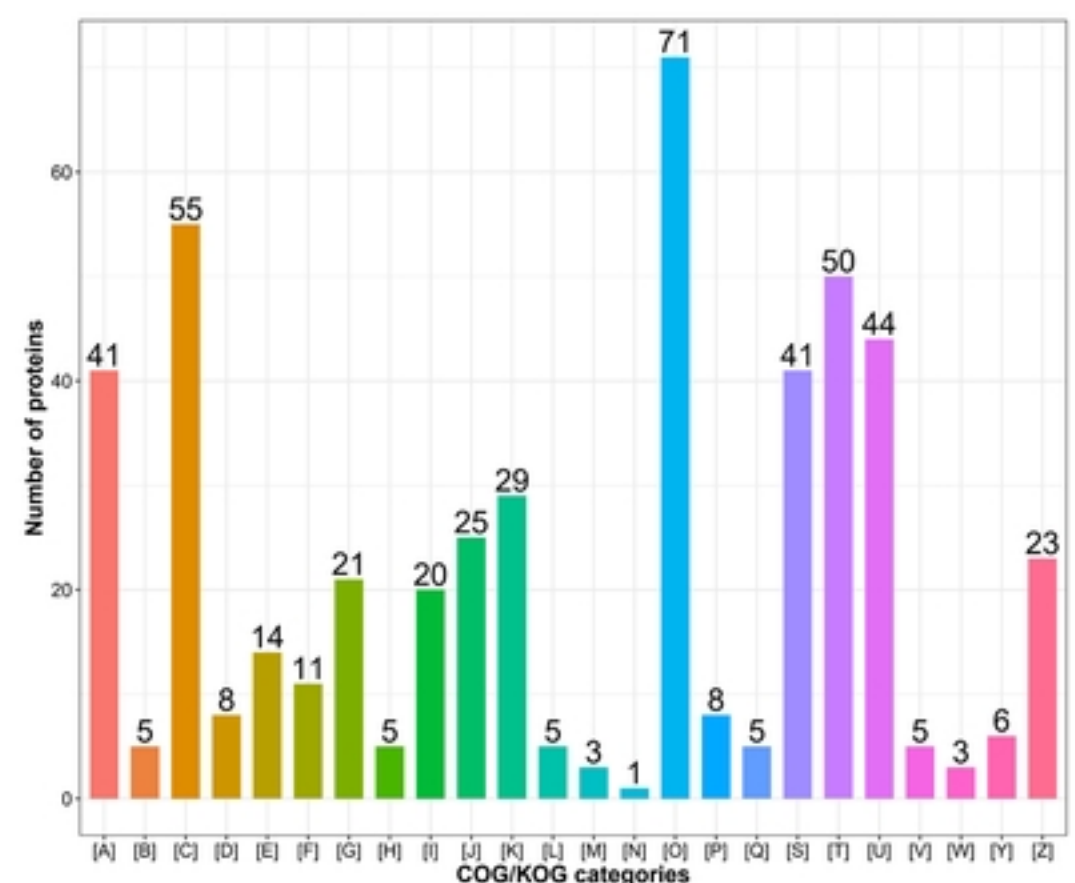
**B**

[A] RNA processing and modification
 [B] Chromatin structure and dynamics
 [C] Energy production and conversion
 [D] Cell cycle control, cell division, chromosome partitioning
 [E] Amino acid transport and metabolism
 [F] Nucleotide transport and metabolism
 [G] Carbohydrate transport and metabolism
 [H] Coenzyme transport and metabolism
 [I] Lipid transport and metabolism
 [J] Translation, ribosomal structure and biogenesis
 [K] Transcription

[O] Posttranslational modification, protein turnover, chaperones
 [P] Inorganic ion transport and metabolism
 [Q] Secondary metabolites biosynthesis, transport and catabolism
 [S] Function unknown
 [T] Signal transduction mechanisms
 [U] Intracellular trafficking, secretion, and vesicular transport
 [V] Defense mechanisms
 [W] Extracellular structures
 [Y] Nuclear structure
 [Z] Cytoskeleton

C**Figure2**

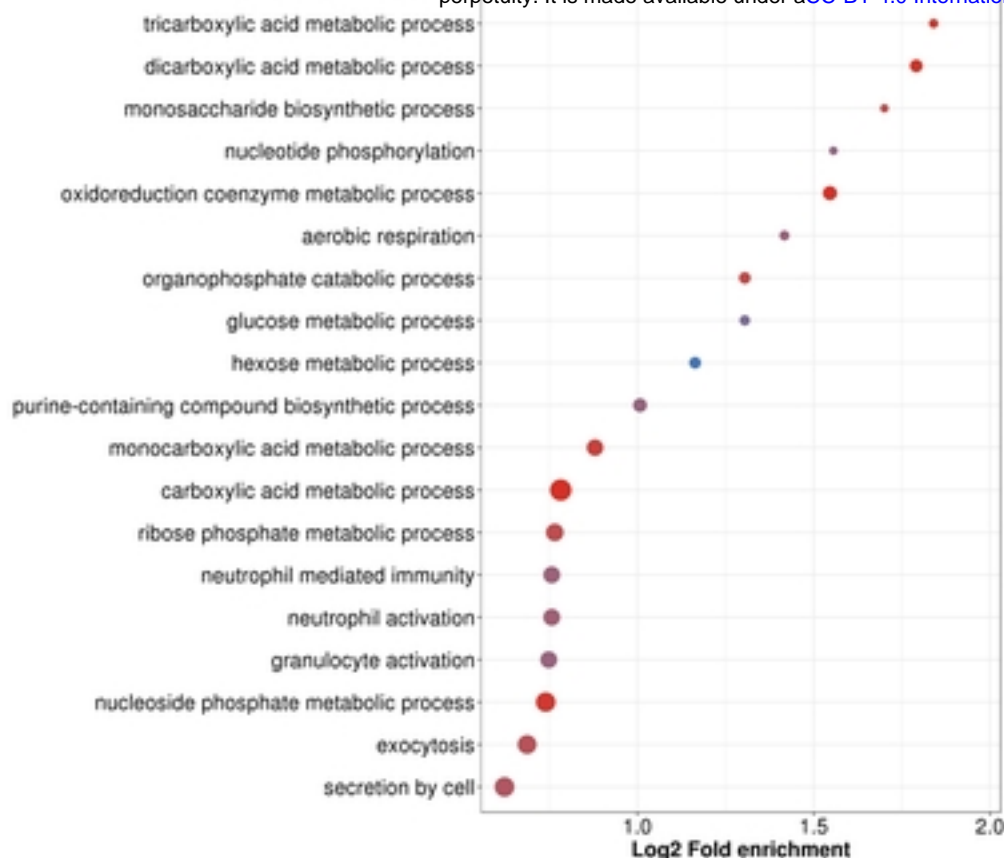
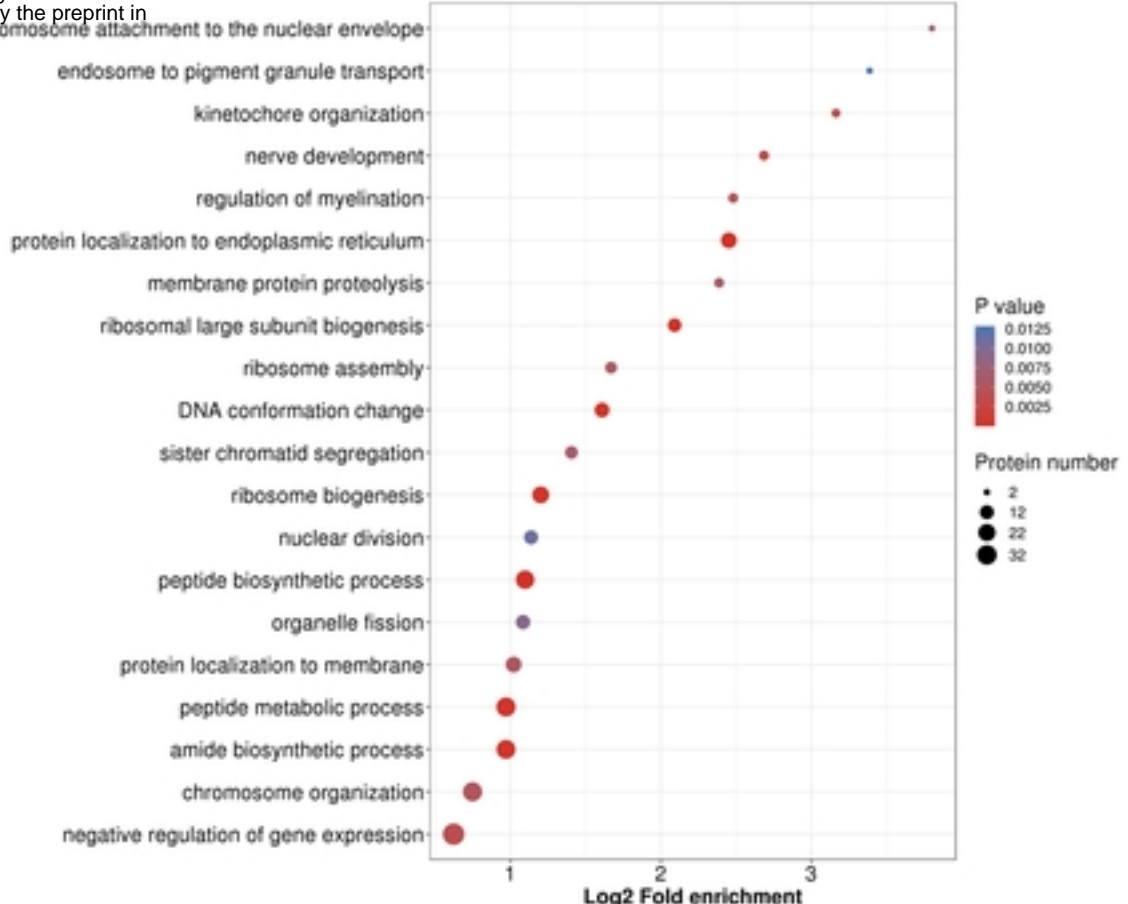
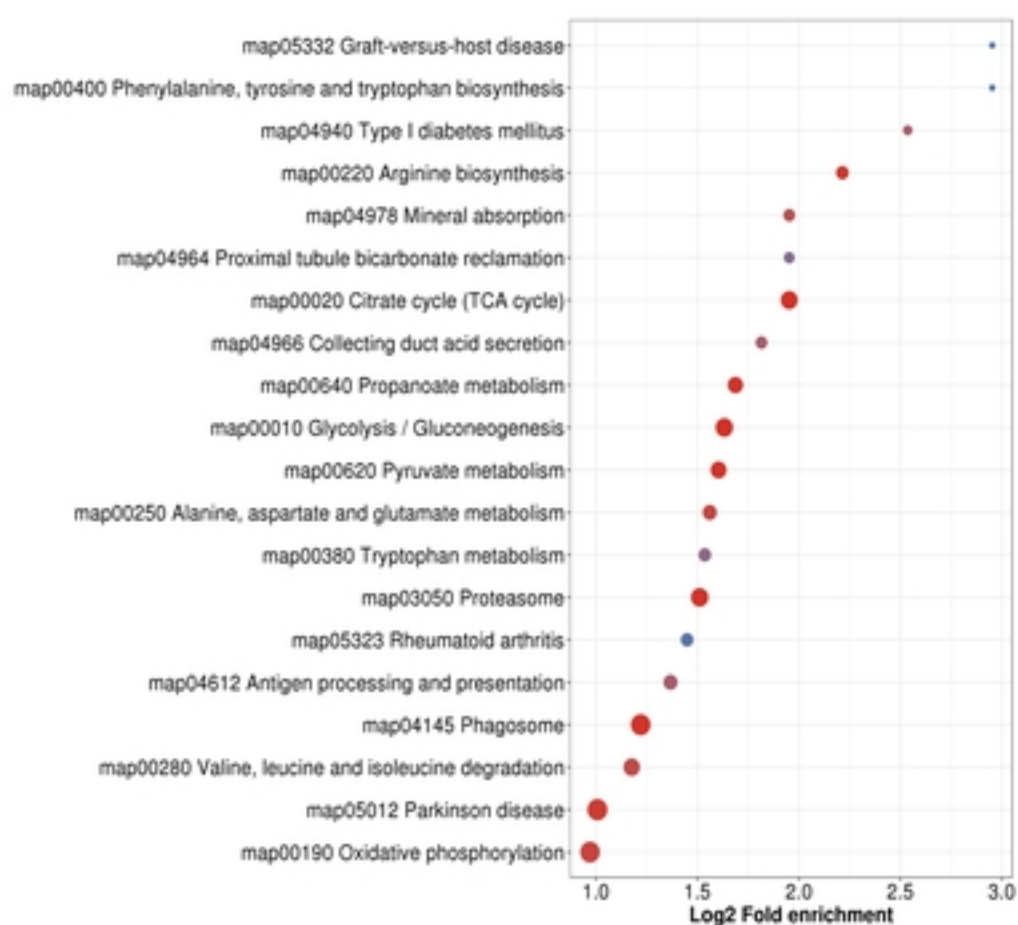
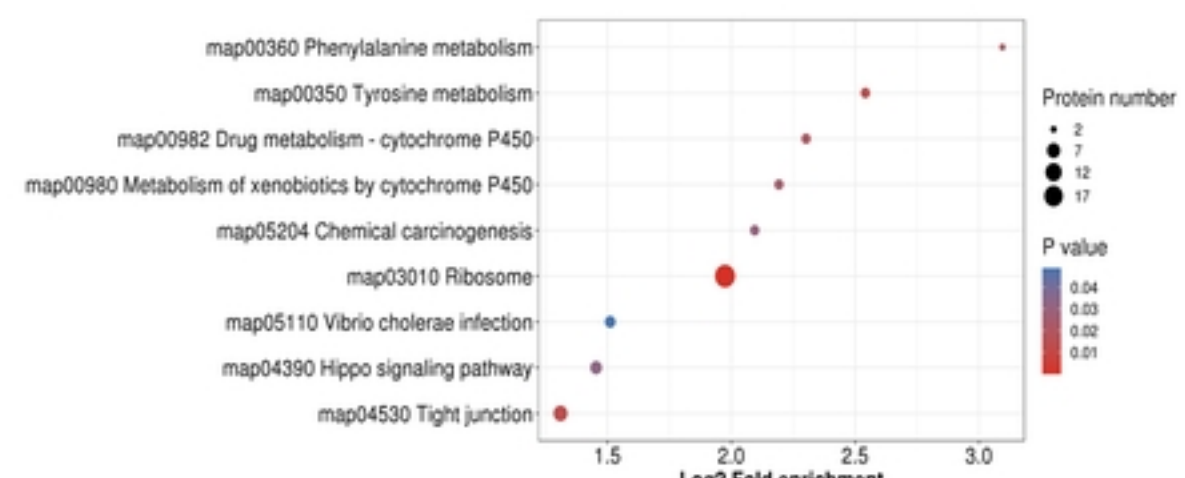
A**B****C****D****Figure3**

A**B****C****D****E****Figure4**

[A] RNA processing and modification
[B] Chromatin structure and dynamics
[C] Energy production and conversion
[D] Cell cycle control, cell division, chromosome partitioning
[E] Amino acid transport and metabolism
[F] Nucleotide transport and metabolism
[G] Carbohydrate transport and metabolism
[H] Coenzyme transport and metabolism
[I] Lipid transport and metabolism
[J] Translation, ribosomal structure and biogenesis
[K] Transcription
[L] Replication, recombination and repair
[M] Cell wall/membrane/envelope biogenesis
[N] Cell motility
[O] Posttranslational modification, protein turnover, chaperones
[P] Inorganic ion transport and metabolism
[Q] Secondary metabolites biosynthesis, transport and catabolism
[S] Function unknown
[T] Signal transduction mechanisms
[U] Intracellular trafficking, secretion, and vesicular transport
[V] Defense mechanisms
[W] Extracellular structures
[Y] Nuclear structure
[Z] Cytoskeleton

A

bioRxiv preprint doi: <https://doi.org/10.1101/2023.01.15.524169>; this version posted January 19, 2023. The copyright holder for this preprint (which was not certified by peer review) is the author/funder, who has granted bioRxiv a license to display the preprint in perpetuity. It is made available under aCC-BY 4.0 International license.

**B****C****D****Figure5**

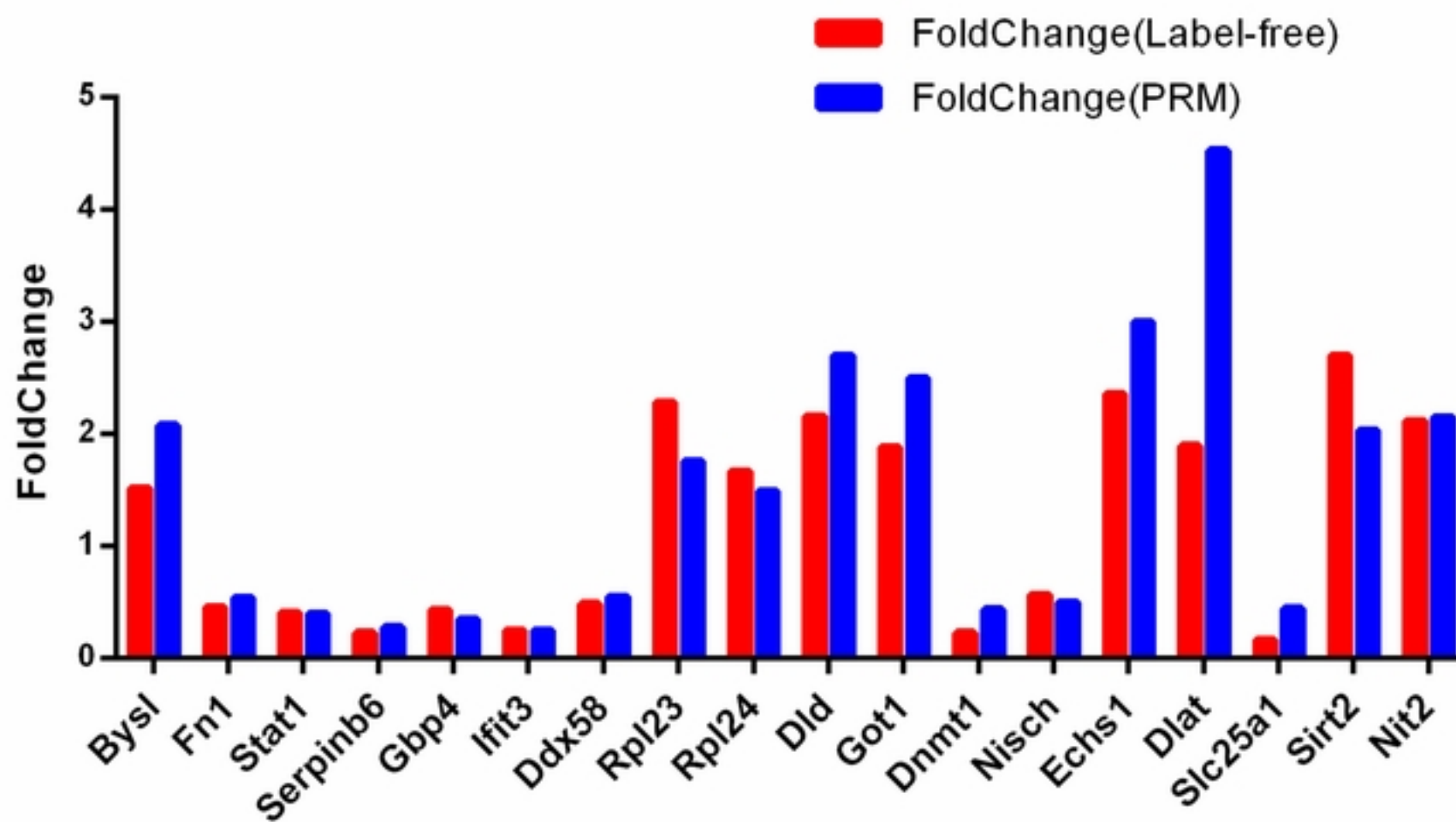


Figure6